

Solid-Phase Synthesis of Boranophosphate/Phosphorothioate/Phosphate Chimeric Oligonucleotides and Their Potential as Antisense Oligonucleotides

Yuhei Takahashi[†], Kazuki Sato^{†}, Takeshi Wada^{†*}*

[†] Department of Medicinal and Life Science, Faculty of Pharmaceutical Sciences,

Tokyo University of Science, 2641 Yamazaki, Noda, Chiba 278-8510, Japan.

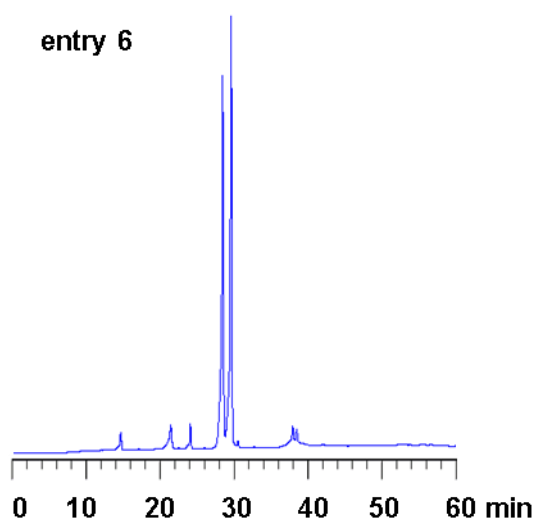
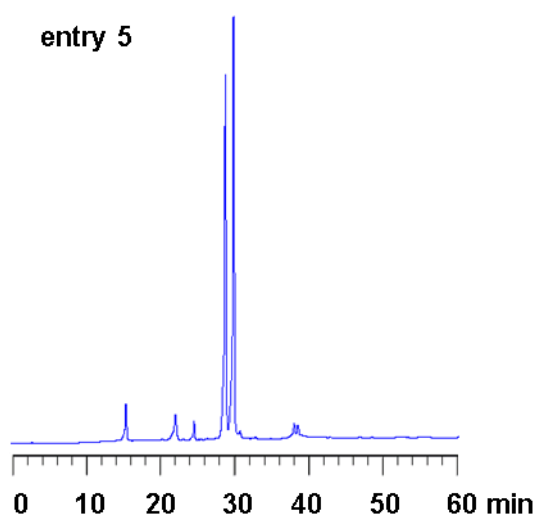
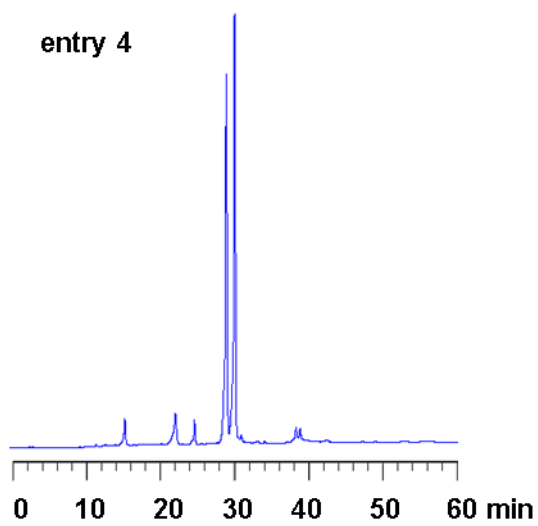
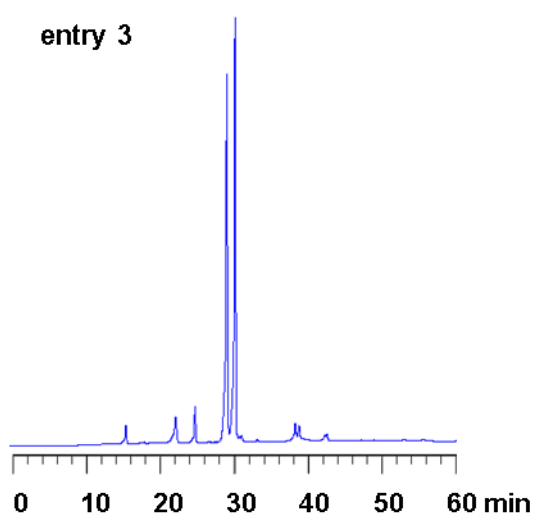
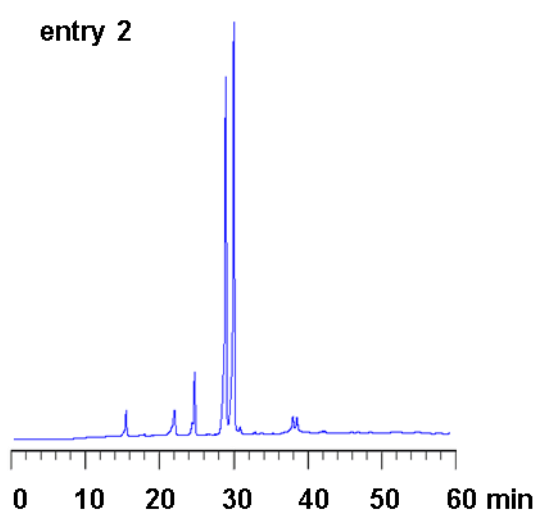
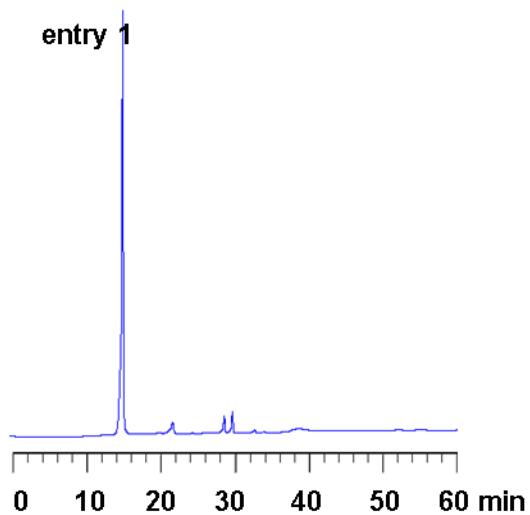
E-mail: kazuki_sato@rs.tus.ac.jp, twada@rs.tus.ac.jp

Support information

Table of Contents

RP-HPLC profiles of T _{PS} T dimer (Figure S1)	S3
RP-HPLC profiles of N _{PS} T dimers (Figure S2)	S5
RP-HPLC profiles of N _{PB} T dimers (Figure S3)	S7
RP-HPLC profiles of tetramers (Figure S4)	S8
RP-HPLC profiles of dodecamers (Figures S5–S18)	S9
Thermal denaturation test (Figure S19–S20)	S19
Nuclease resistance (Figure S21)	S21
RNase H activity (25 U/mL, Figure S22)	S24
RNase H activity (50 U/mL, Figure S23)	S26
NMR spectra	S28

RP-HPLC profiles of T_{PS}T dimer (Table 1)



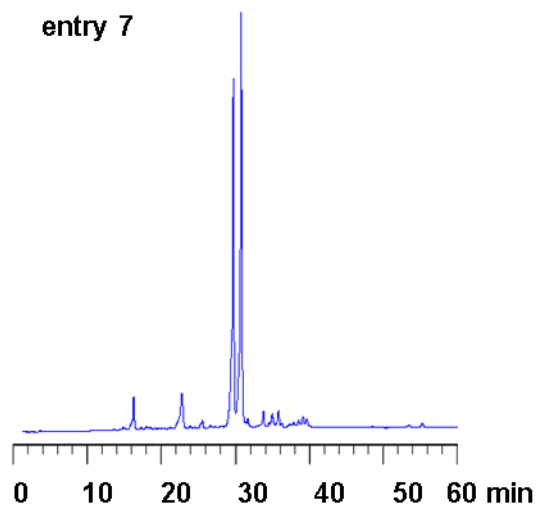
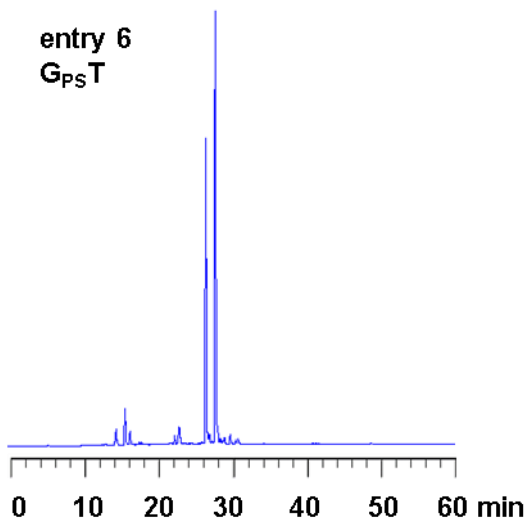
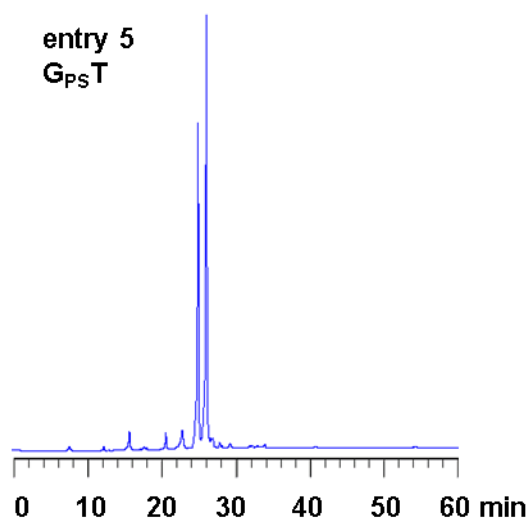
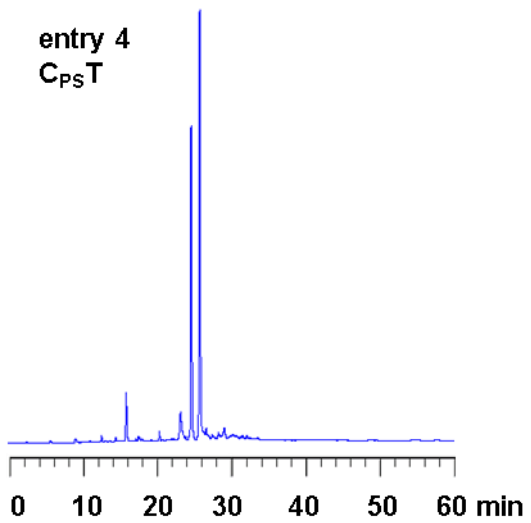
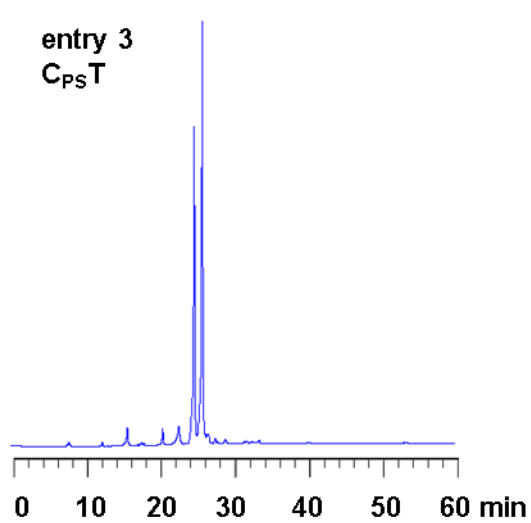
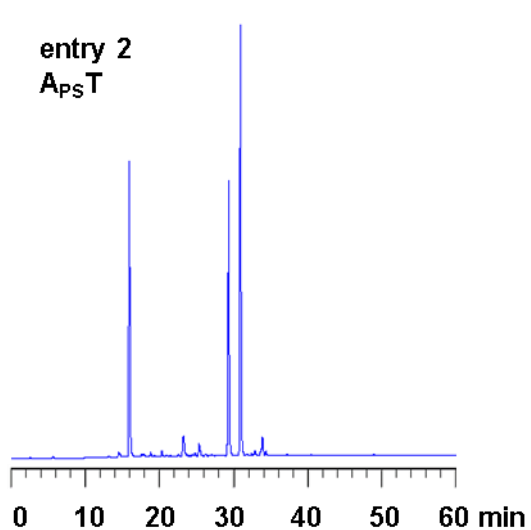
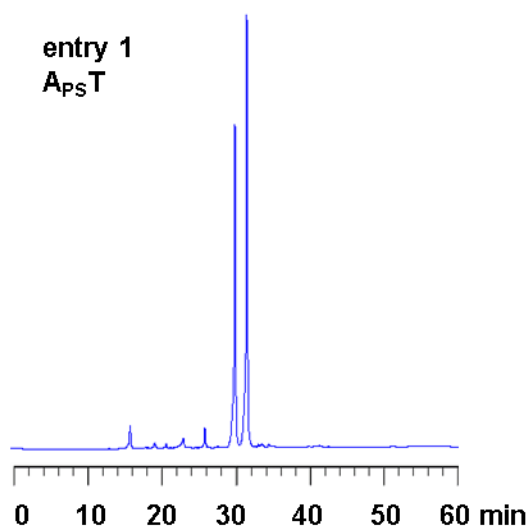


Figure S1. RP-HPLC profiles of crude T_{PS}T. RP-HPLC was performed with a linear gradient of 0%–30% acetonitrile for 60 min in 0.1 M triethylammonium acetate buffer (pH 7.0) at 30 °C at a flow rate of 0.5 mL/min using a C18 column.

RP-HPLC profiles of B_{PS}T dimers (Table 2)



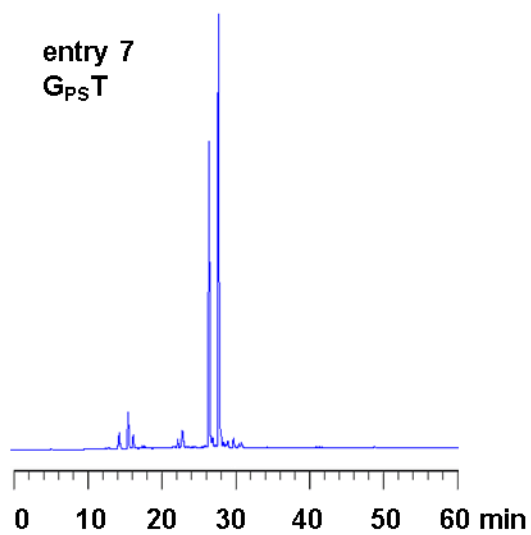


Figure S2. RP-HPLC profiles of crude B_{PS}T. RP-HPLC was performed with a linear gradient of 0%–30% acetonitrile for 60 min in 0.1 M triethylammonium acetate buffer (pH 7.0) at 30 °C at a flow rate of 0.5 mL/min using a C18 column.

RP-HPLC profiles of B_{PB}T dimers (Table 3)

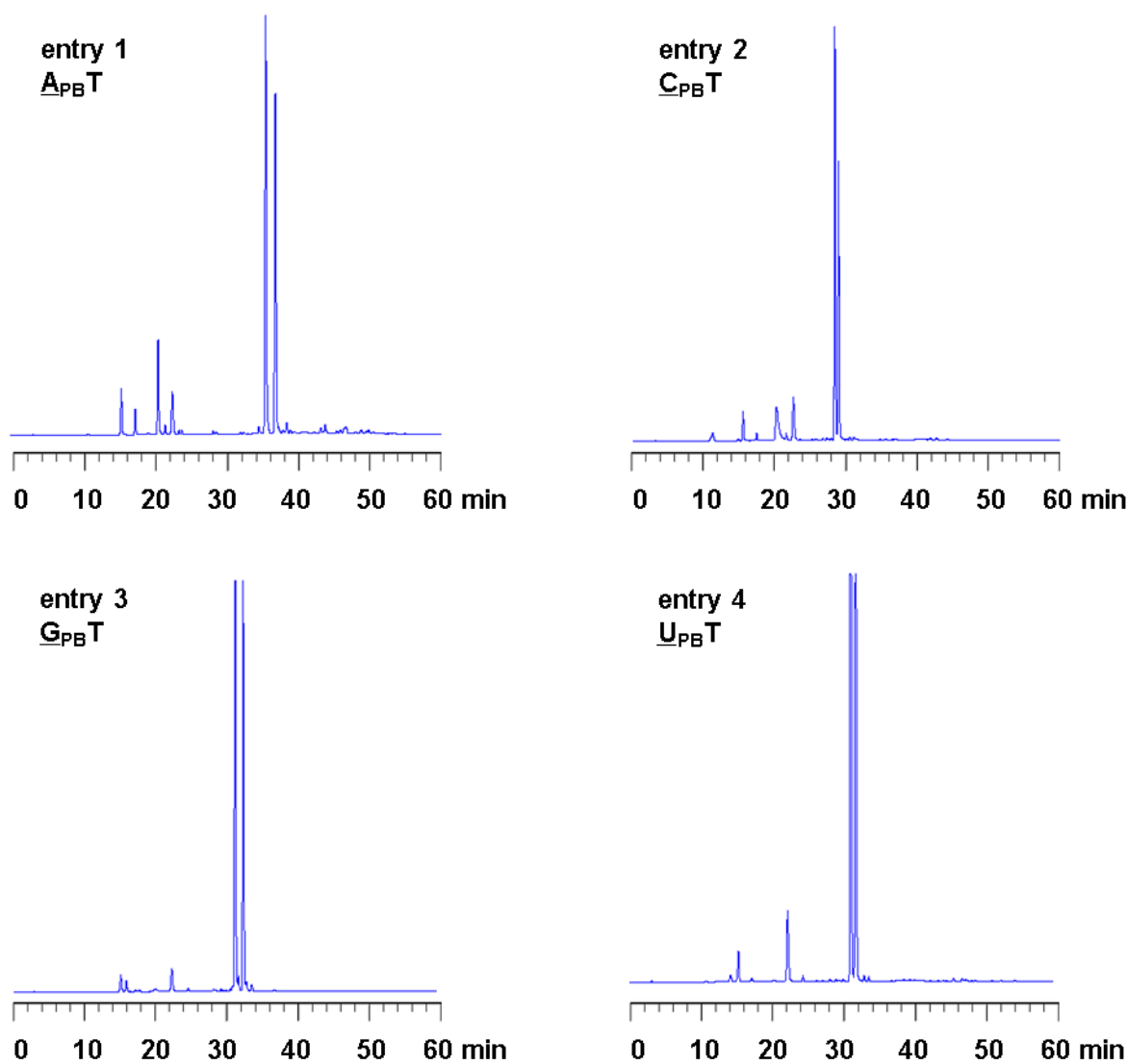


Figure S3. RP-HPLC profiles of crude B_{PB}T. RP-HPLC was performed with a linear gradient of 0%–30% acetonitrile for 60 min in 0.1 M triethylammonium acetate buffer (pH 7.0) at 30 °C at a flow rate of 0.5 mL/min using a C18 column.

RP-HPLC profiles of tetramers (Table 4, entries 1 and 2)

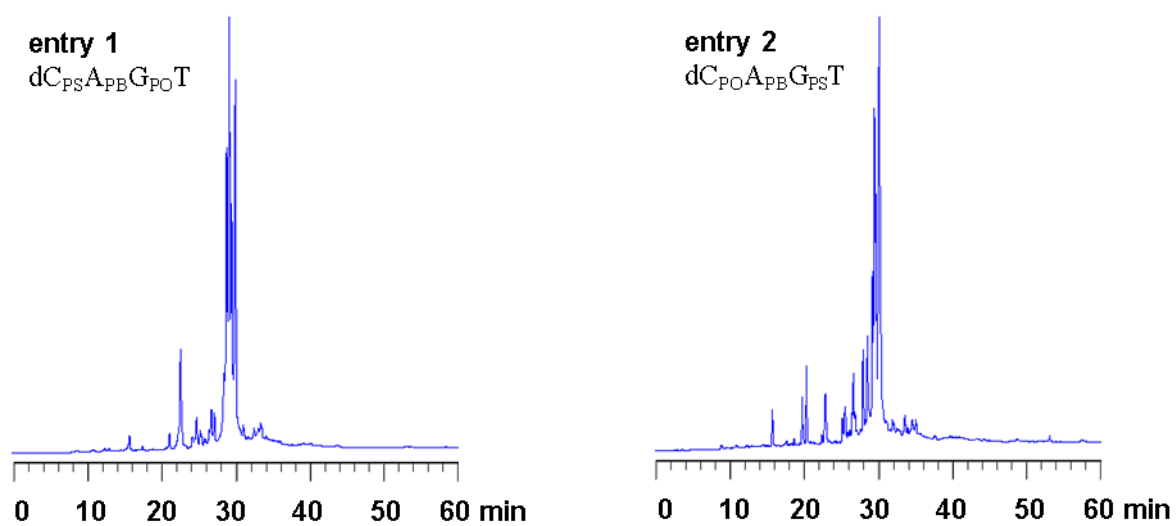


Figure S4. RP-HPLC profiles of crude tetramers (dC_{PS}A_{PB}G_{PO}T and dC_{PO}A_{PB}G_{PS}T). RP-HPLC was performed with a linear gradient of 0%–30% acetonitrile for 60 min in 0.1 M triethylammonium acetate buffer (pH 7.0) at 30 °C at a flow rate of 0.5 mL/min using a C18 column.

HPLC profiles of dodecamers (Table 4 entry 3)

crude

dC_{PS}A_{PS}G_{PS}T_{PS}C_{PB}A_{PB}G_{PB}T_{PB}C_{PO}A_{PO}G_{PO}T

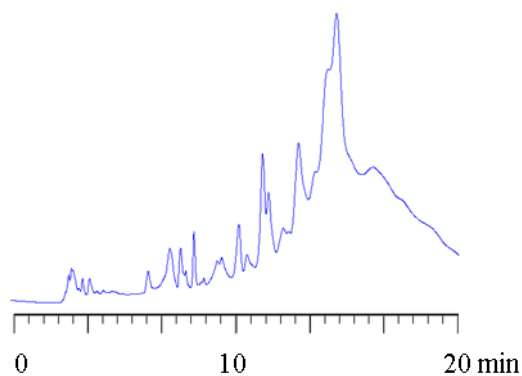


Figure S5. RP-HPLC profile of crude dC_{PS}A_{PS}G_{PS}T_{PS}C_{PB}A_{PB}G_{PB}T_{PB}C_{PO}A_{PO}G_{PO}T. RP-HPLC was performed with a linear gradient of 5%–40% MeOH in 100 mM HFIP, 8 mM TEA for 20 min at 60 °C at a flow rate of 0.5 mL/min using a C18 column.

pure

dC_{PS}A_{PS}G_{PS}T_{PS}C_{PB}A_{PB}G_{PB}T_{PB}C_{PO}A_{PO}G_{PO}T

RP-HPLC

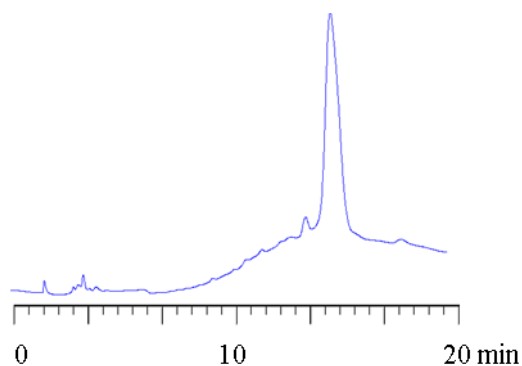


Figure S6. RP-HPLC profile of pure dC_{PS}A_{PS}G_{PS}T_{PS}C_{PB}A_{PB}G_{PB}T_{PB}C_{PO}A_{PO}G_{PO}T. RP-HPLC was performed with a linear gradient of 5%–40% MeOH in 100 mM HFIP, 8 mM TEA for 20 min at 60 °C at a flow rate of 0.5 mL/min using a C18 column.

pure
dC_{PS}A_{PS}G_{PS}T_{PS}C_{PB}A_{PB}G_{PB}T_{PB}C_{PO}A_{PO}G_{PO}T
IE-HPLC

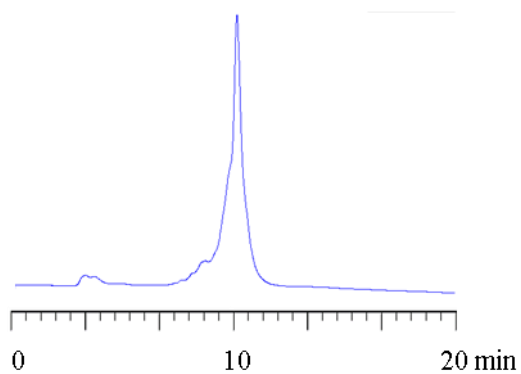


Figure S7. IE-HPLC profile of pure dC_{PS}A_{PS}G_{PS}T_{PS}C_{PB}A_{PB}G_{PB}T_{PB}C_{PO}A_{PO}G_{PO}T. IE-HPLC was performed with a linear gradient of 0 M–1M NaClO₄ in 50%–25% CH₃CN, 10 mM Tris-HCl (pH 7.5) for 20 min at 30 °C with a flow rate of 0.4 mL/min using a quaternary ammonium anion exchange resin column.

HPLC profiles of dodecamers (Table 4 entry 4)

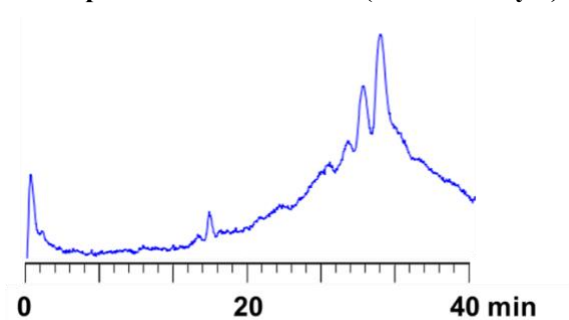


Figure S8. IE-HPLC profile of crude $dG_{PB}C_{PS}A_{PB}T_{PO}T_{PO}G_{PO}G_{PO}T_{PS}A_{PB}T_{PS}T_{PB}C$. IE-HPLC was performed with a linear gradient of 0 M–1 M NaCl in 30% *i*PrOH, 10 mM Tris-HCl (pH 7.5) for 40 min at a flow rate of 0.4 mL/min using a quaternary ammonium anion exchange resin column.

pure
 $dG_{PB}C_{PS}A_{PB}T_{PO}T_{PO}G_{PO}G_{PO}T_{PS}A_{PB}T_{PS}T_{PB}C$
RP-HPLC

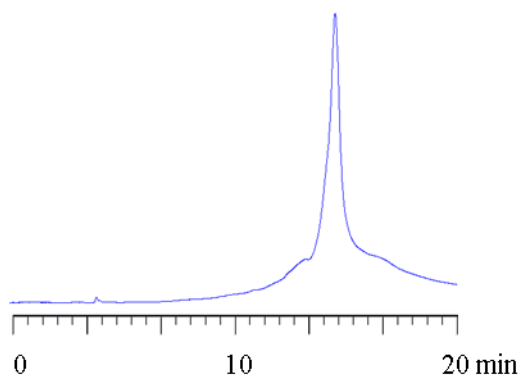


Figure S9. RP-HPLC profile of pure $dG_{PB}C_{PS}A_{PB}T_{PO}T_{PO}G_{PO}G_{PO}T_{PS}A_{PB}T_{PS}T_{PB}C$. RP-HPLC was performed with a linear gradient of 5%–40% MeOH in 100 mM HFIP, 8 mM TEA for 20 min at 60 °C at a flow rate of 0.5 mL/min using a C18 column.

pure
dC_{PS}A_{PS}G_{PS}T_{PS}C_{PB}A_{PB}G_{PB}T_{PB}C_{PO}A_{PO}G_{PO}T
IE-HPLC

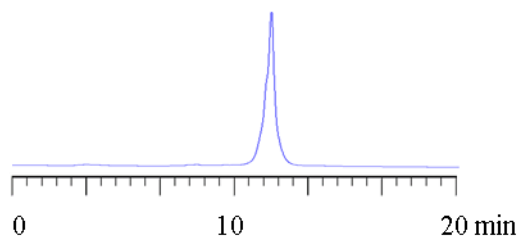


Figure S9. IE-HPLC profile of pure dG_{PB}C_{PS}A_{PB}T_{PO}T_{PO}G_{PO}G_{PO}T_{PS}A_{PB}T_{PS}T_{PB}C. IE-HPLC was performed with a linear gradient of 0 M–1 M NaClO₄ in 50%–25% CH₃CN, 10 mM Tris-HCl (pH 7.5) for 20 min at 30 °C with a flow rate of 0.4 mL/min using a quaternary ammonium anion exchange resin column.

HPLC profiles of dodecamers (Table 4 entry 5)

crude

$dG_{PB}C_{PS}A_{PB}T_{PS}T_{PS}G_{PB}G_{PB}T_{PS}A_{PB}T_{PS}T_{PB}C$

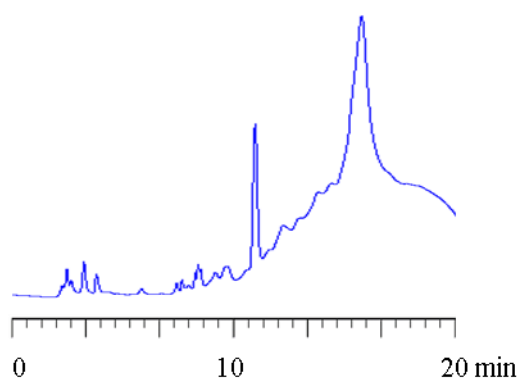


Figure S10. RP-HPLC profile of crude $dG_{PB}C_{PS}A_{PB}T_{PS}T_{PS}G_{PB}G_{PB}T_{PS}A_{PB}T_{PS}T_{PB}C$. RP-HPLC was performed with a linear gradient of 5%–40% MeOH in 100 mM HFIP, 8 mM TEA for 20 min at 60 °C at a flow rate of 0.5 mL/min using a C18 column.

pure

$dG_{PB}C_{PS}A_{PB}T_{PS}T_{PS}G_{PB}G_{PB}T_{PS}A_{PB}T_{PS}T_{PB}C$
RP-HPLC

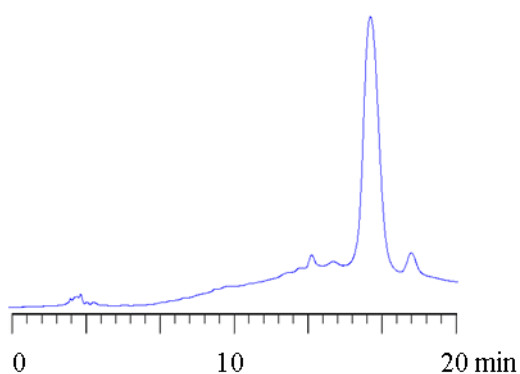


Figure S11. RP-HPLC profile of pure $dG_{PB}C_{PS}A_{PB}T_{PS}T_{PS}G_{PB}G_{PB}T_{PS}A_{PB}T_{PS}T_{PB}C$. RP-HPLC was performed with a linear gradient of 5%–40% MeOH in 100 mM HFIP, 8 mM TEA for 20 min at 60 °C at a flow rate of 0.5 mL/min using a C18 column.

pure
dG_{PB}C_{PS}A_{PB}T_{PS}T_{PS}G_{PB}G_{PB}T_{PS}A_{PB}T_{PS}T_{PB}C
IE-HPLC

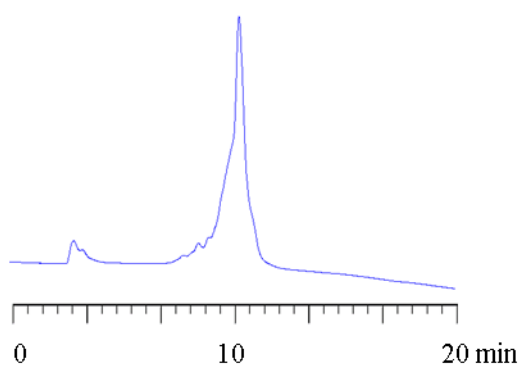


Figure S12. IE-HPLC profile of pure dG_{PB}C_{PS}A_{PB}T_{PS}T_{PS}G_{PB}G_{PB}T_{PS}A_{PB}T_{PS}T_{PB}C. IE-HPLC was performed with a linear gradient of 0 M–1 M NaClO₄ in 50%–25% CH₃CN, 10 mM Tris-HCl (pH 7.5) for 20 min at 30 °C with a flow rate of 0.4 mL/min using a quaternary ammonium anion exchange resin column.

HPLC profiles of dodecamers (Table 4 entry 6)

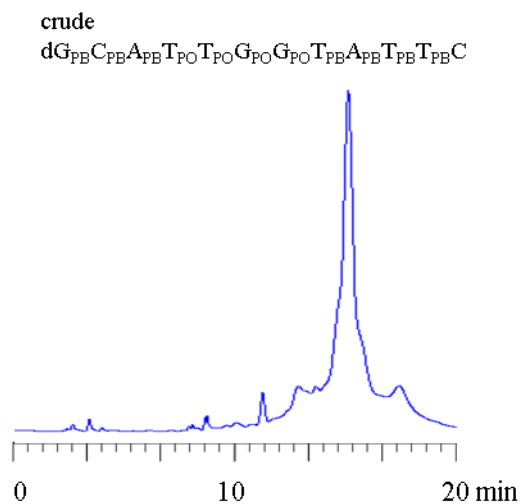


Figure S13. RP-HPLC profile of crude dG_{PB}C_{PB}A_{PB}T_{PO}T_{PO}G_{PO}G_{PO}T_{PB}A_{PB}T_{PB}T_{PB}C. RP-HPLC was performed with a linear gradient of 5%–40% MeOH in 100 mM HFIP, 8 mM TEA for 20 min at 60 °C at a flow rate of 0.5 mL/min using a C18 column.

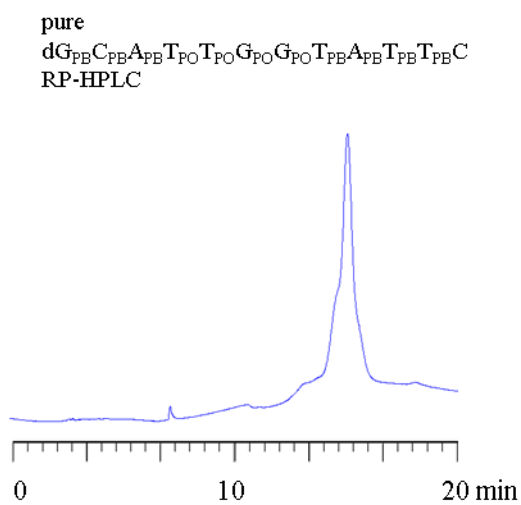


Figure S14. RP-HPLC profile of pure dG_{PB}C_{PB}A_{PB}T_{PO}T_{PO}G_{PO}G_{PO}T_{PB}A_{PB}T_{PB}T_{PB}C. RP-HPLC was performed with a linear gradient of 5%–40% MeOH in 100 mM HFIP, 8 mM TEA for 20 min at 60 °C at a flow rate of 0.5 mL/min using a C18 column.

pure
dG_{PB}C_{PB}A_{PB}T_{PO}T_{PO}G_{PO}G_{PO}T_{PB}A_{PB}T_{PB}T_{PB}C
IE-HPLC

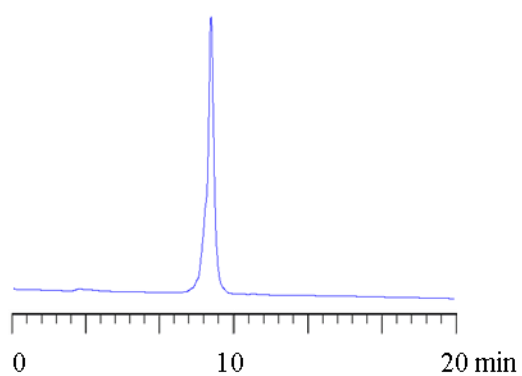


Figure S15. IE-HPLC profile of pure dG_{PB}C_{PB}A_{PB}T_{PO}T_{PO}G_{PO}G_{PO}T_{PB}A_{PB}T_{PB}T_{PB}C. IE-HPLC was performed with a linear gradient of 0 M–1 M NaClO₄ in 50%–25% CH₃CN, 10 mM Tris-HCl (pH 7.5) for 20 min at 30 °C with a flow rate of 0.4 mL/min using a quaternary ammonium anion exchange resin column.

HPLC profiles of dodecamers (Table 4 entry 7)

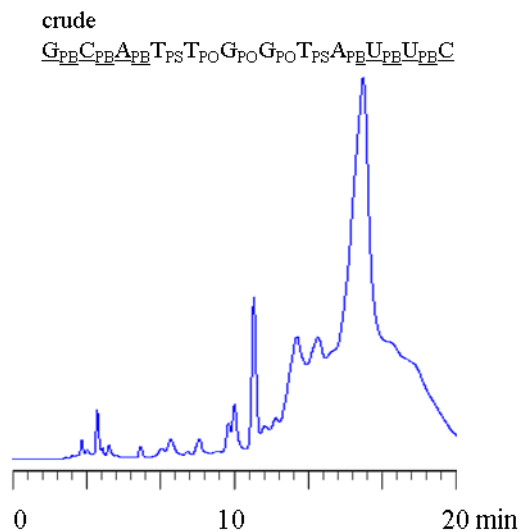


Figure S16. RP-HPLC profile of crude G_{PE}C_{PE}A_{PE}T_{PS}T_{PO}G_{PO}G_{PO}T_{PS}A_{PE}U_{PE}U_{PE}C. RP-HPLC was performed with a linear gradient of 5%–40% MeOH in 100 mM HFIP, 8 mM TEA for 20 min at 60 °C at a flow rate of 0.5 mL/min using a C18 column.

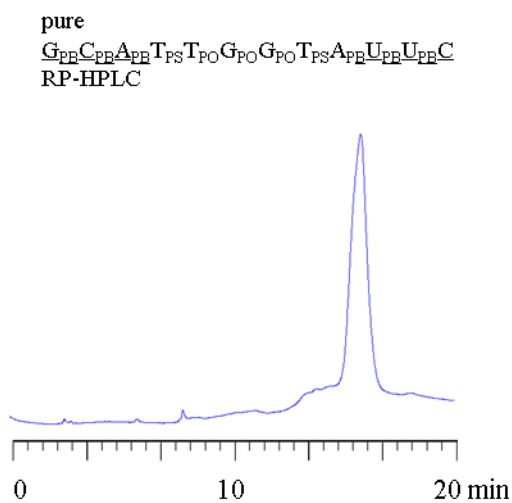


Figure S17. RP-HPLC profile of pure G_{PE}C_{PE}A_{PE}T_{PS}T_{PO}G_{PO}G_{PO}T_{PS}A_{PE}U_{PE}U_{PE}C. RP-HPLC was performed with a linear gradient of 5%–40% MeOH in 100 mM HFIP, 8 mM TEA for 20 min at 60 °C at a flow rate of 0.5 mL/min using a C18 column.

pure G_{PB}C_{PB}A_{PB}T_{PS}T_{PO}G_{PO}G_{PO}T_{PS}A_{PB}U_{PB}U_{PB}C
IE-HPLC

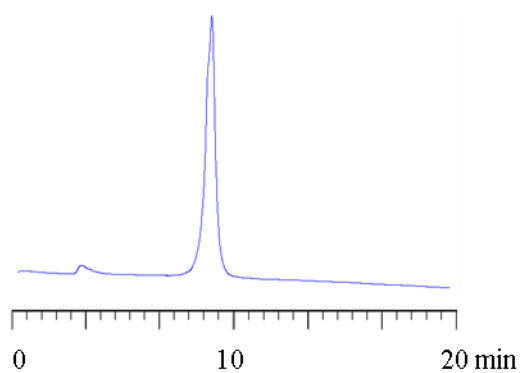


Figure S18. IE-HPLC profile of pure G_{PB}C_{PB}A_{PB}T_{PS}T_{PO}G_{PO}G_{PO}T_{PS}A_{PB}U_{PB}U_{PB}C. IE-HPLC was performed with a linear gradient of 0 M–1 M NaClO₄ in 50%–25% CH₃CN, 10 mM Tris-HCl (pH 7.5) for 20 min at 30 °C with a flow rate of 0.4 mL/min using a quaternary ammonium anion exchange resin column.

Thermal denaturation test

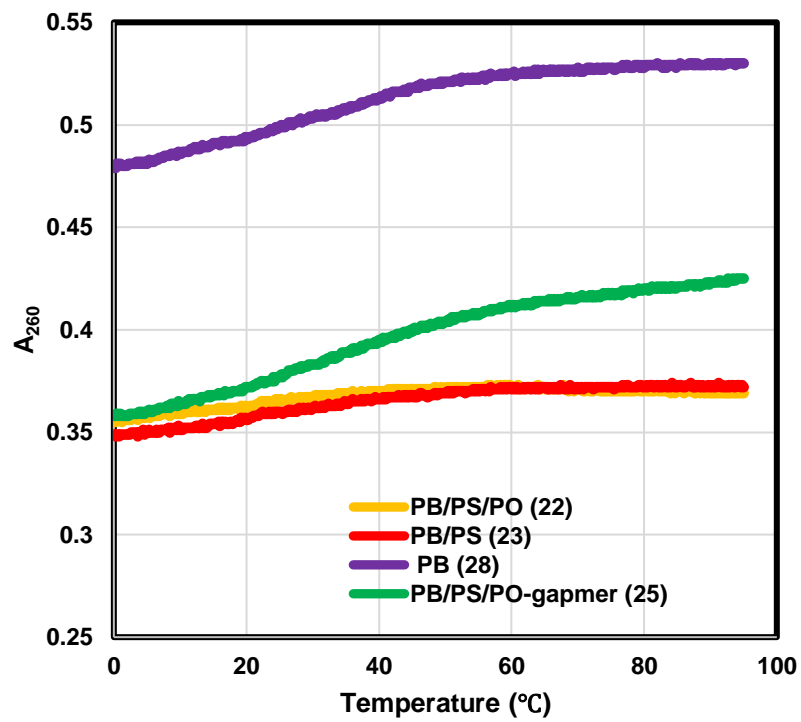


Figure S19. UV Melting curves of single stranded ODNs 22, 23, 25, and 28.

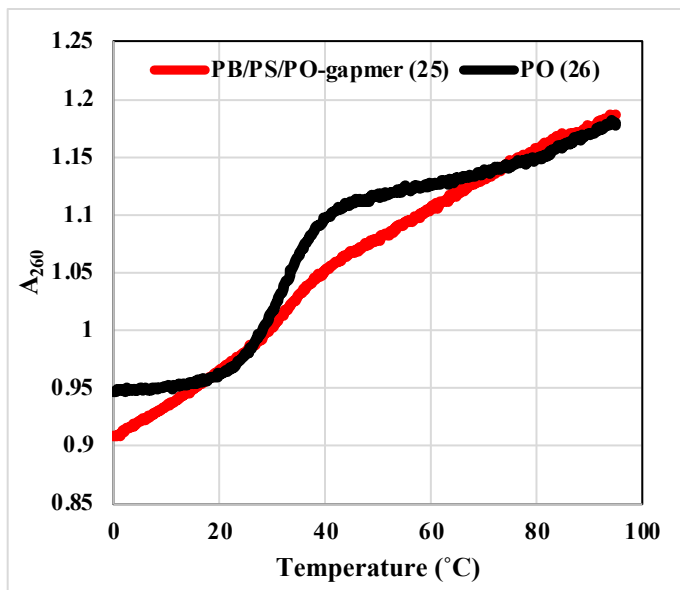
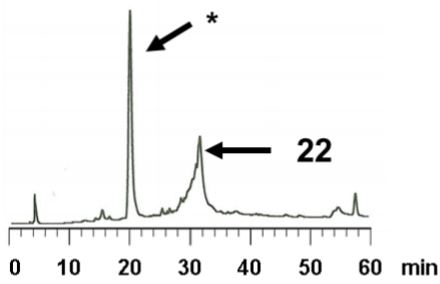


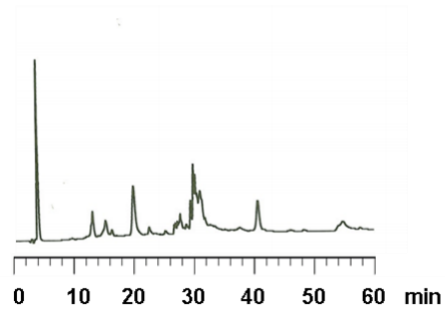
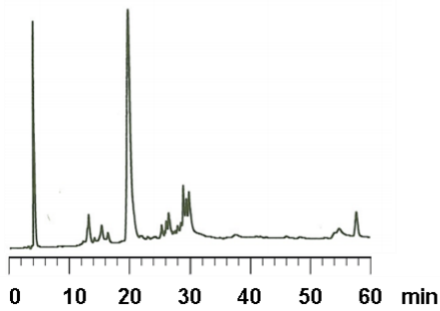
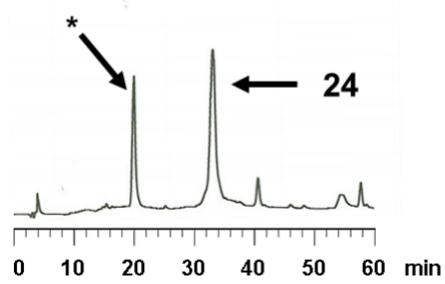
Figure S20. UV Melting curves of double stranded ODNs 25 and 26 with cRNA with a mismatched base.

Nuclease resistance

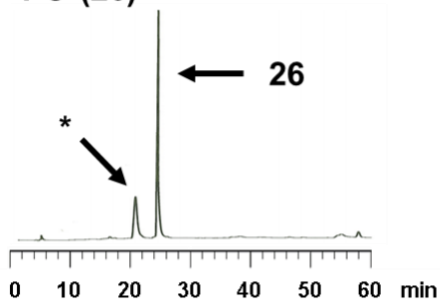
PB/PS/PO (22)



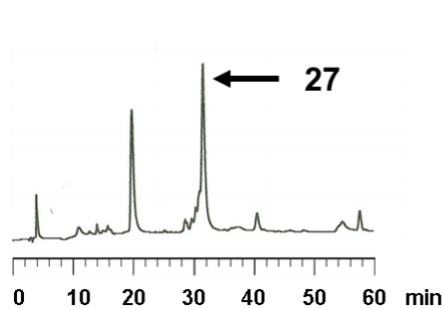
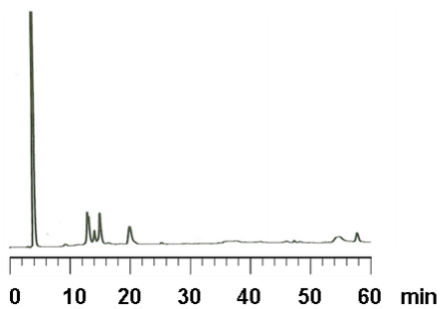
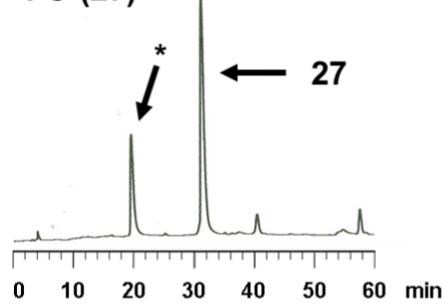
PB/PO (24)

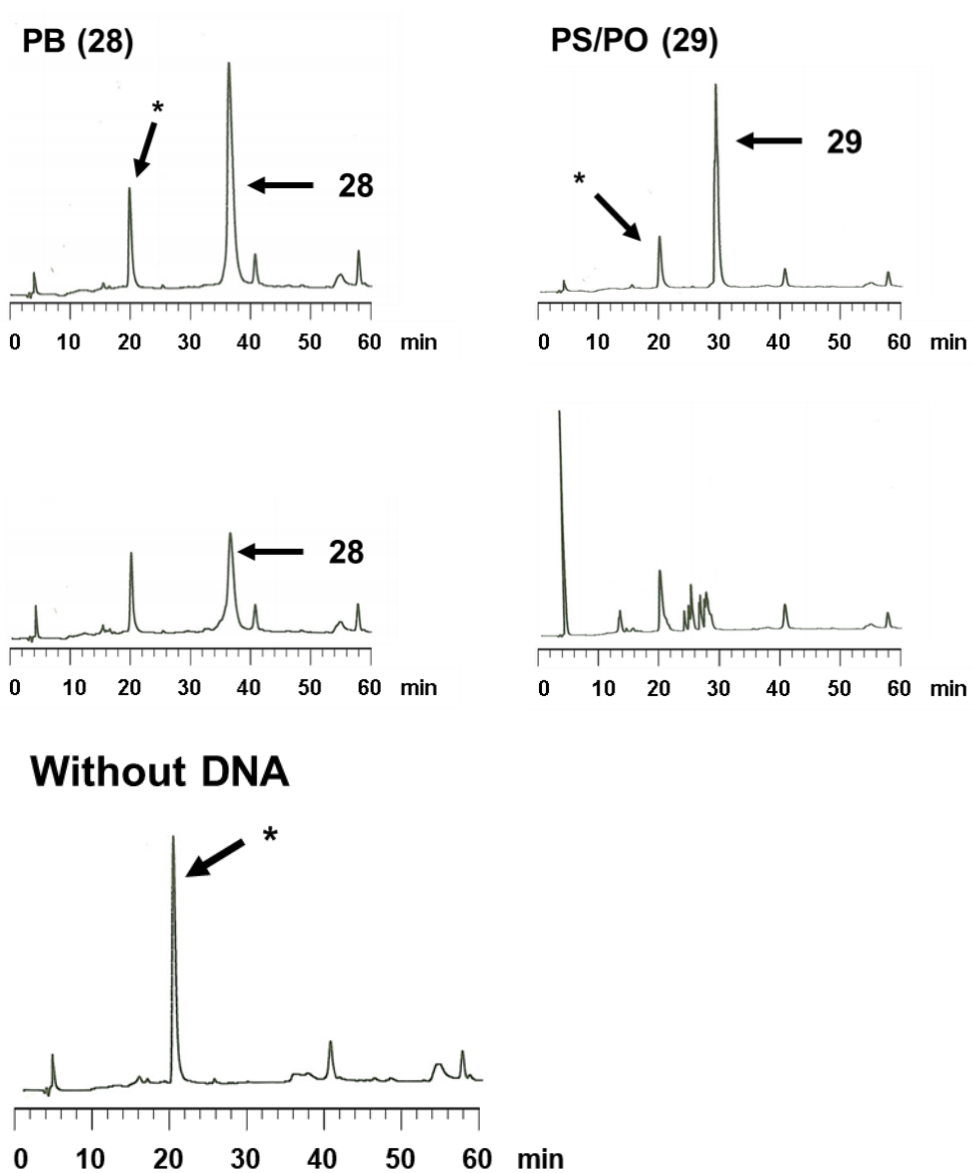


PO (26)



PS (27)

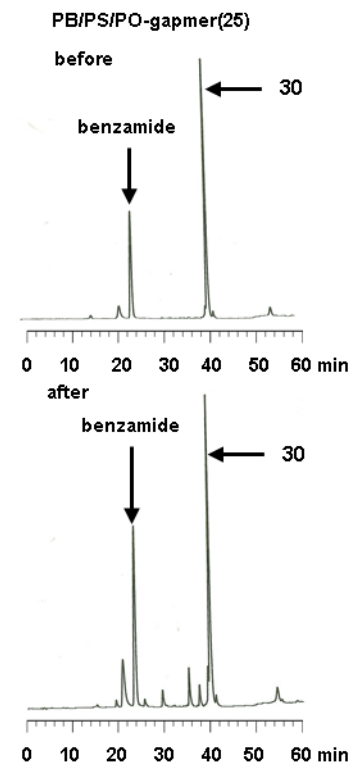
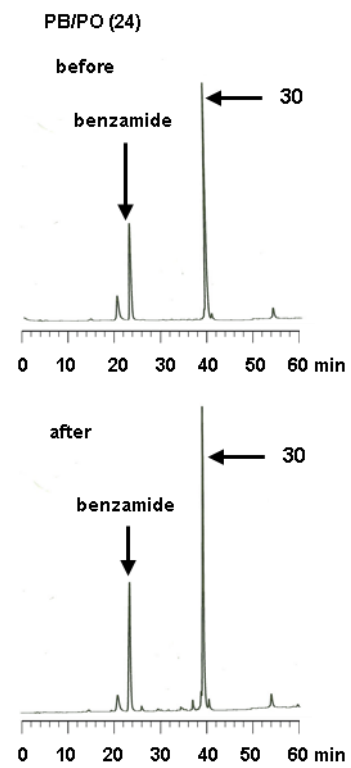
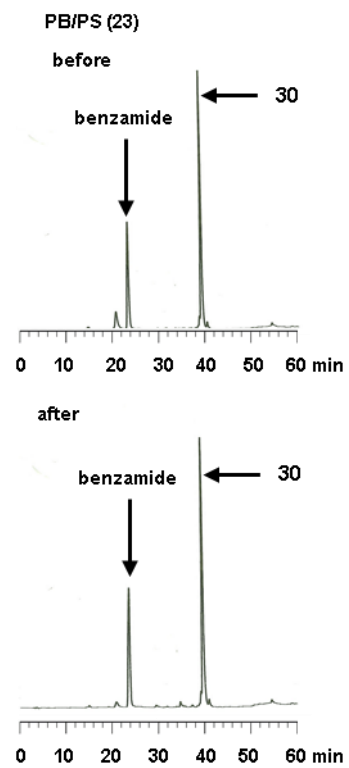
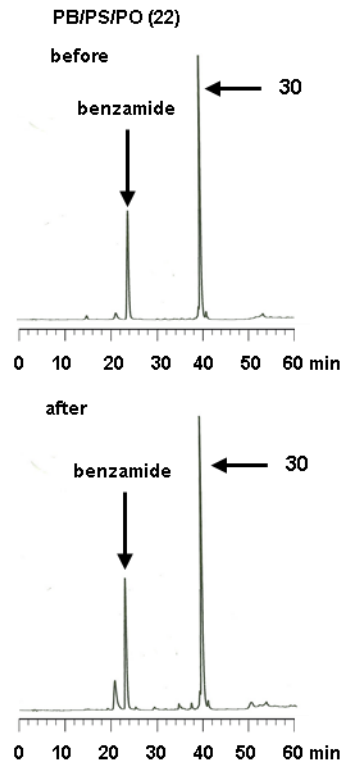




* indicates an artifact peak

Figure S21. RP-HPLC profiles of ODN before (upper) and after (lower) the treatment with snake venom phosphodiesterase (SVPDE) for 12 h at 37°C. RP-HPLC was performed with a linear gradient of 0%–40% acetonitrile for 60 min in 0.1 M triethylammonium acetate buffer (pH 7.0) at 30 °C at a flow rate of 0.5 mL/min using a C18 column

RNase H activity (25 U/mL)



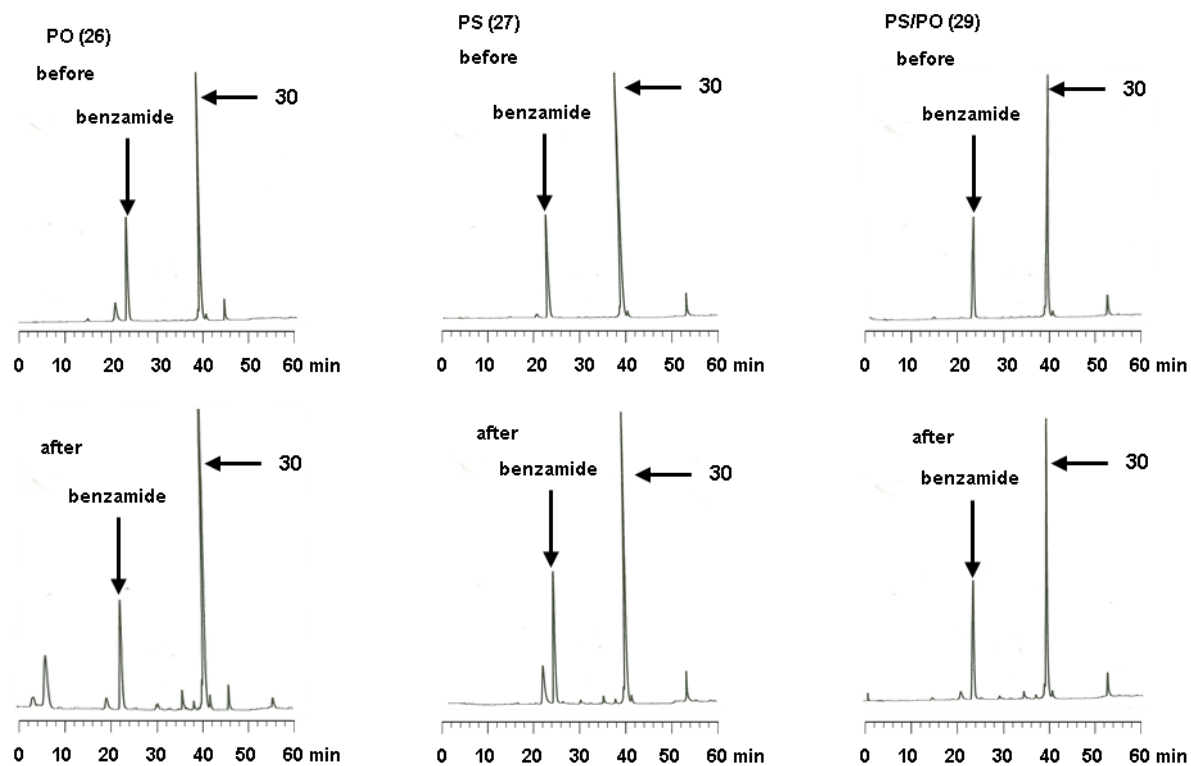
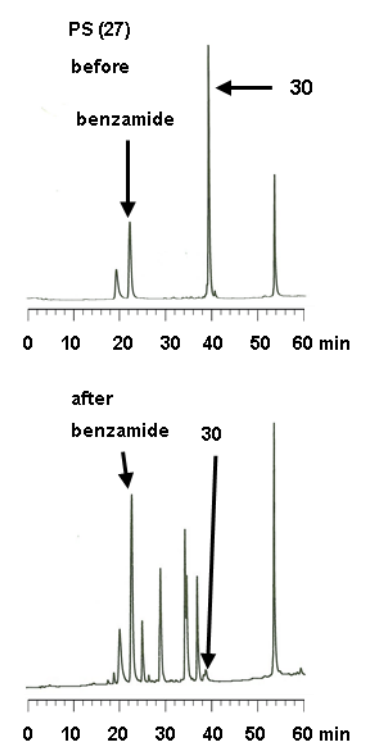
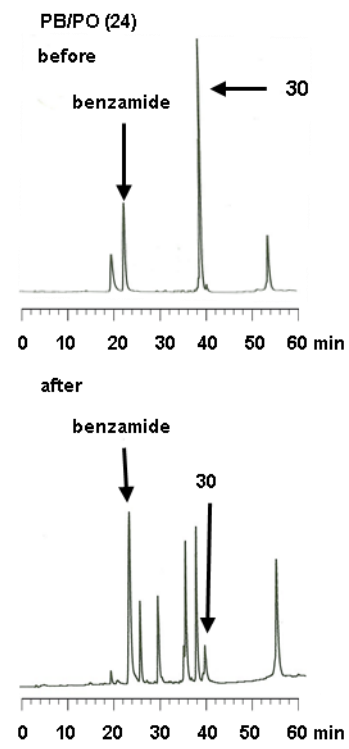
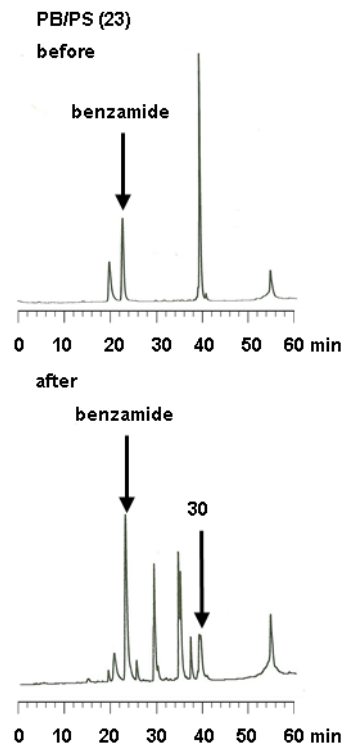
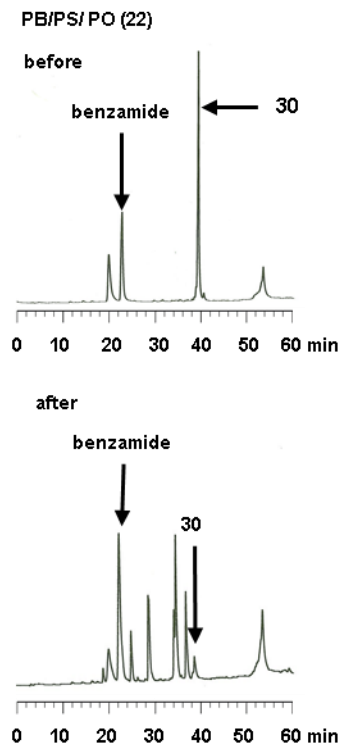


Figure S22. RP-HPLC profiles of ODN/cRNA duplexes before (upper) and after (lower) the treatment with 25 U/mL RNase H for 30 min at 37 °C RP-HPLC was performed with a linear gradient of 0%–11% MeCN over 44 min followed by 11–40% over 16 min in 0.1 M TEAA buffer (pH 7.0) at 50 °C with a flow rate of 0.5 mL/min.

RNase H activity (50 U/mL)



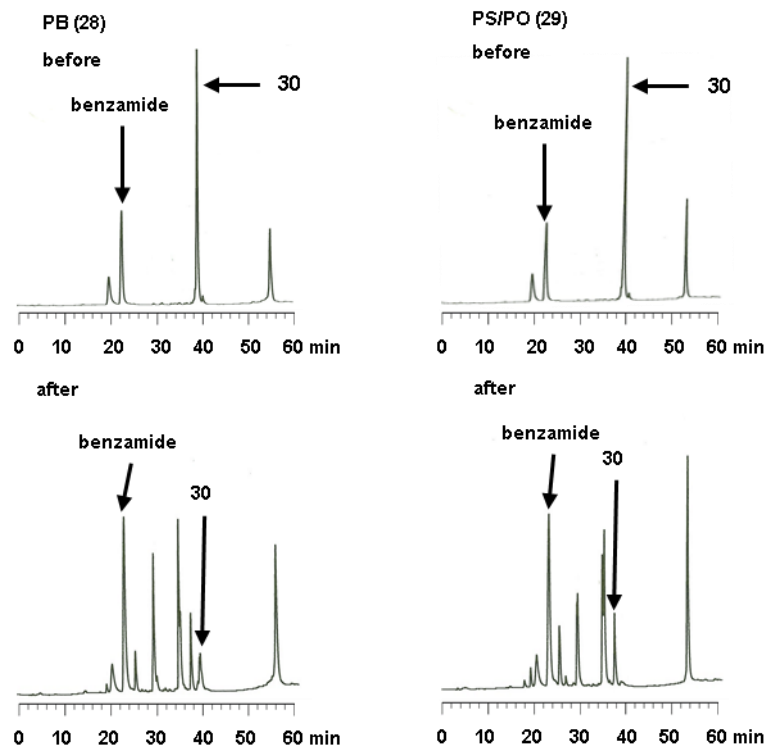
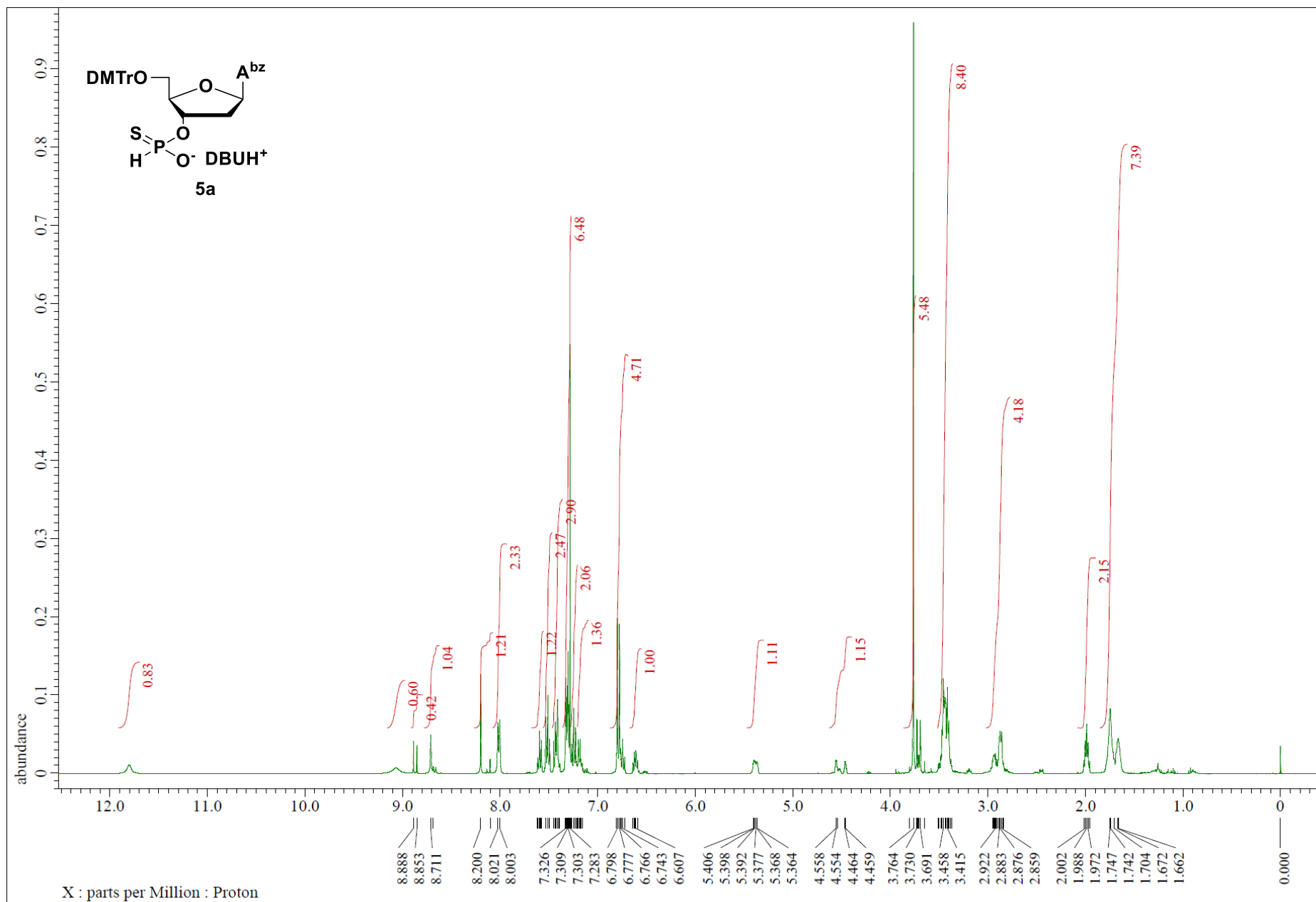


Figure S23. RP-HPLC profiles of ODN/cRNA duplexes before (upper) and after (lower) the treatment with 50 U/mL RNase H for 30 min at 37 °C RP-HPLC was performed with a linear gradient of 0%–11% MeCN over 44 min followed by 11%–40% over 16 min in 0.1 M TEAA buffer (pH 7.0) at 50 °C with a flow rate of 0.5 mL/min.

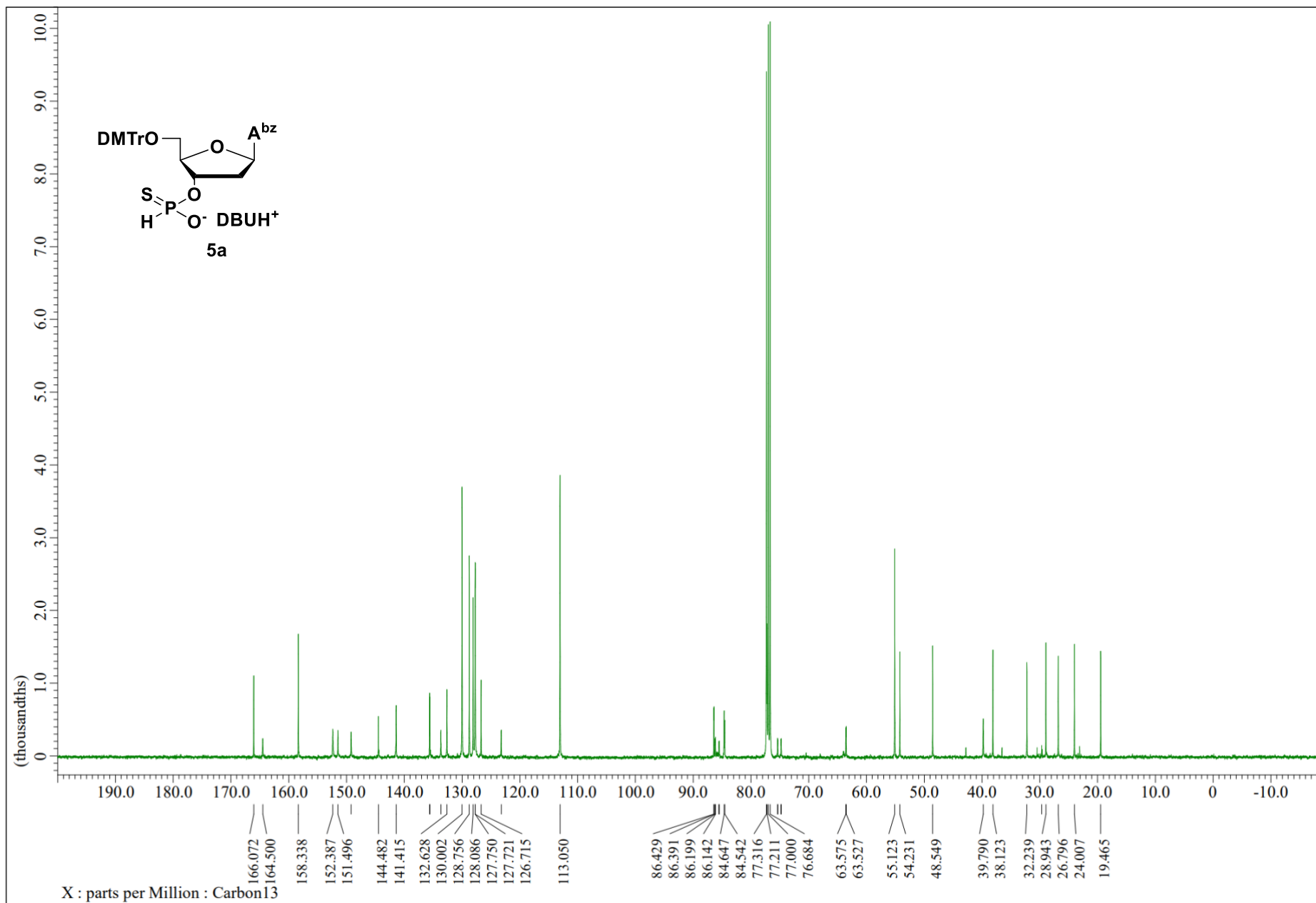
^1H , ^{13}C , ^{31}P NMR spectra

NMR spectra

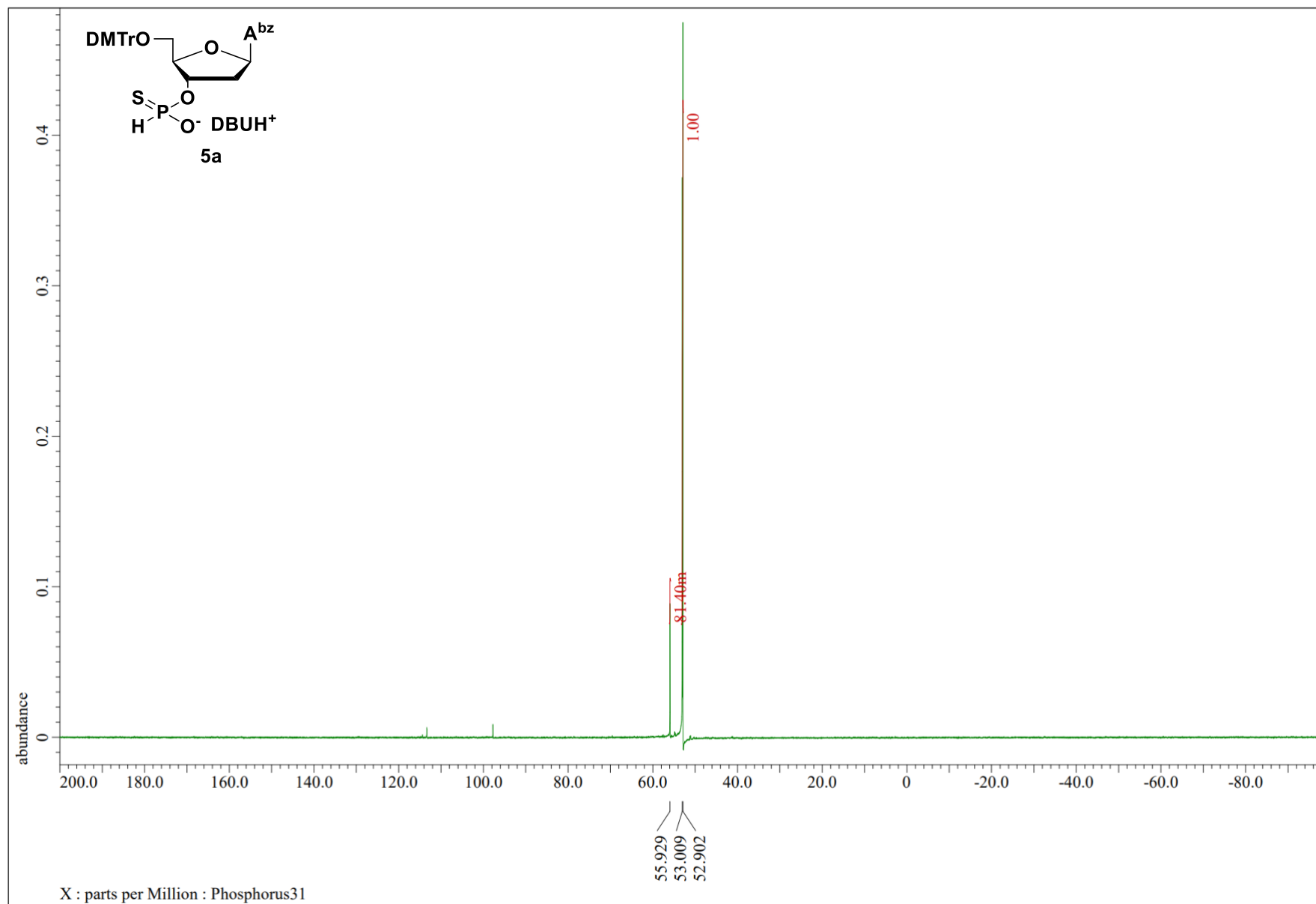
^1H -NMR (400 MHz, CDCl_3)



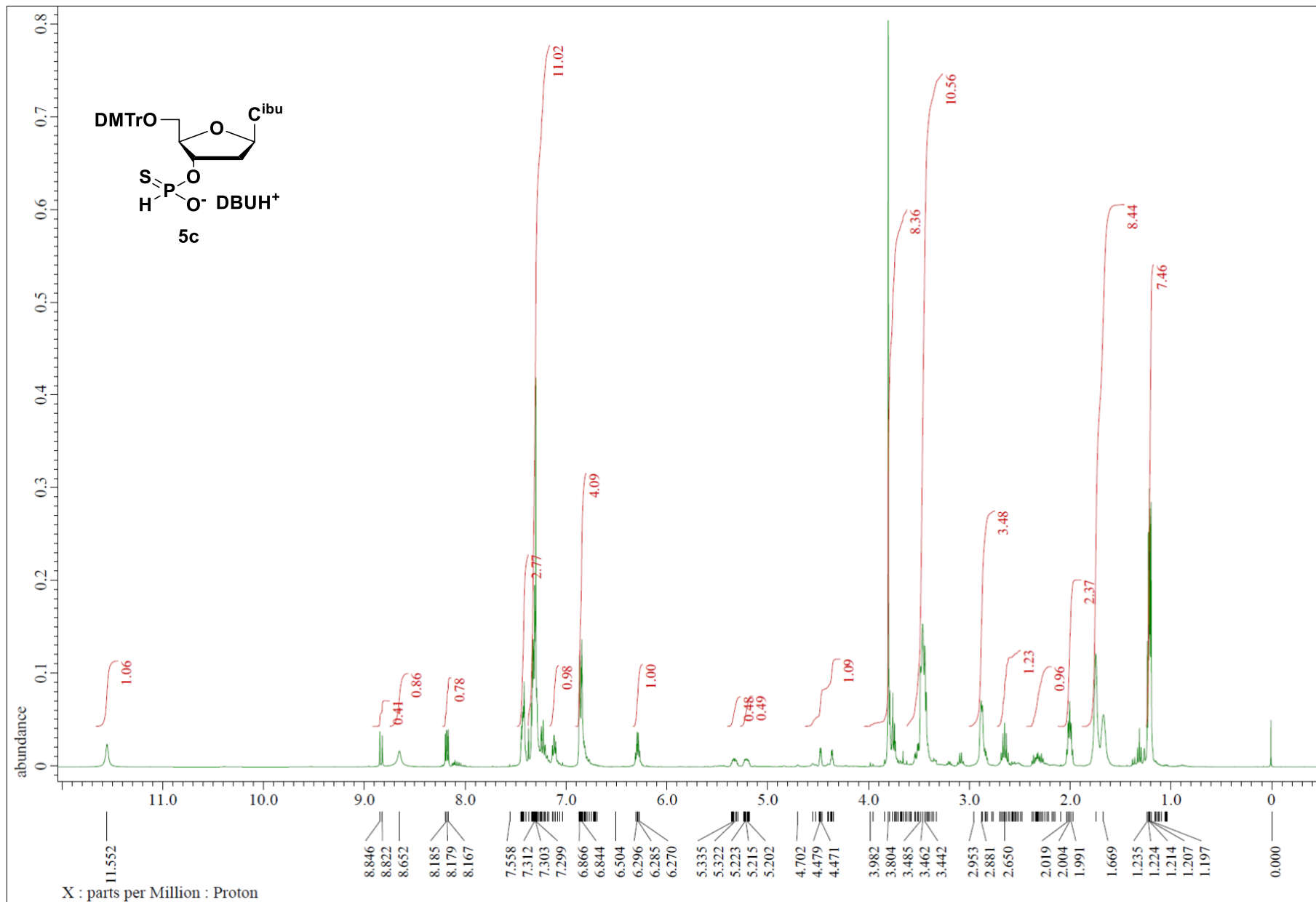
$^{13}\text{C}\{^1\text{H}\}$ NMR (100 MHz, CDCl_3)

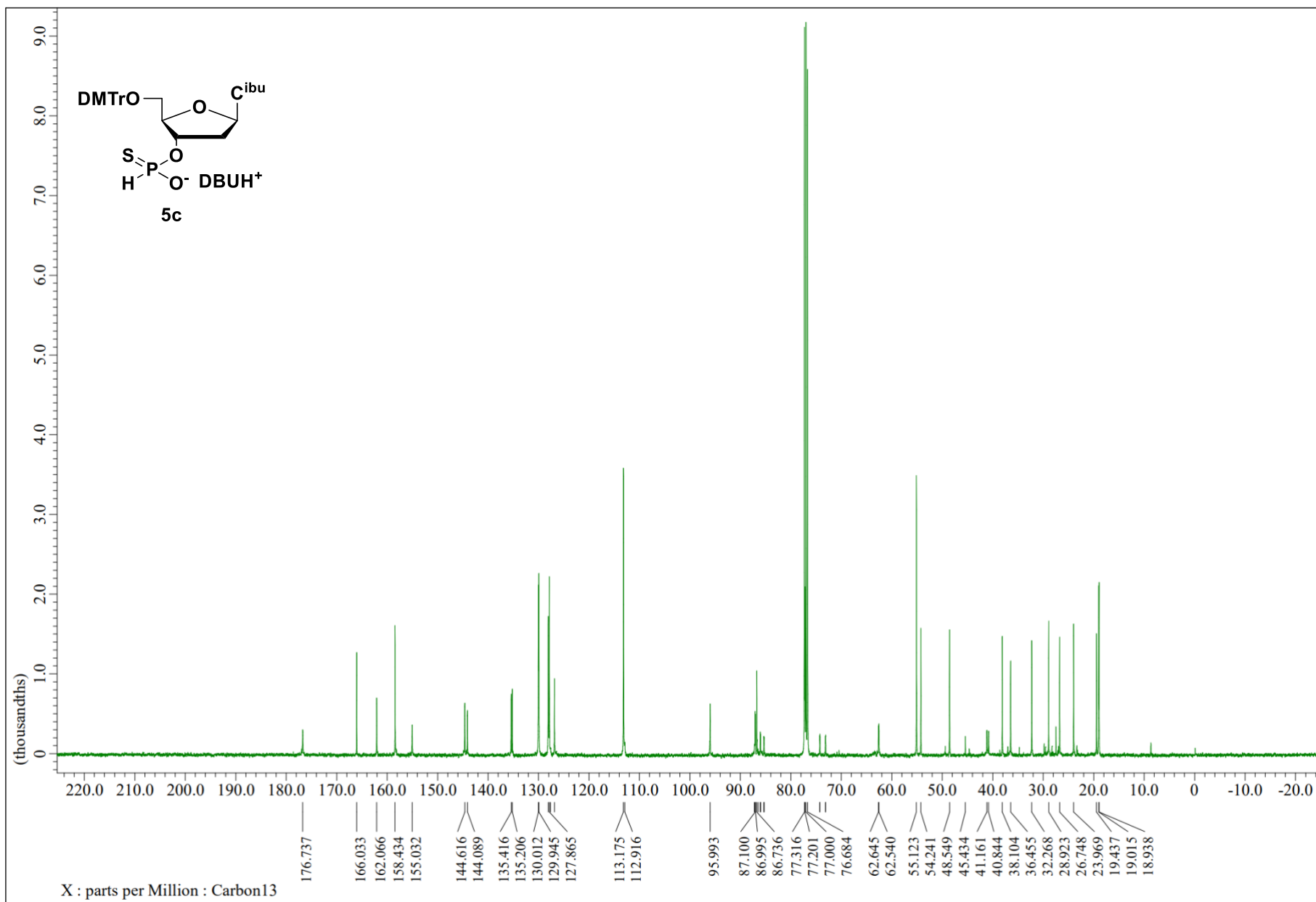


$^{31}\text{P}\{^1\text{H}\}$ NMR (162 MHz, CDCl_3)

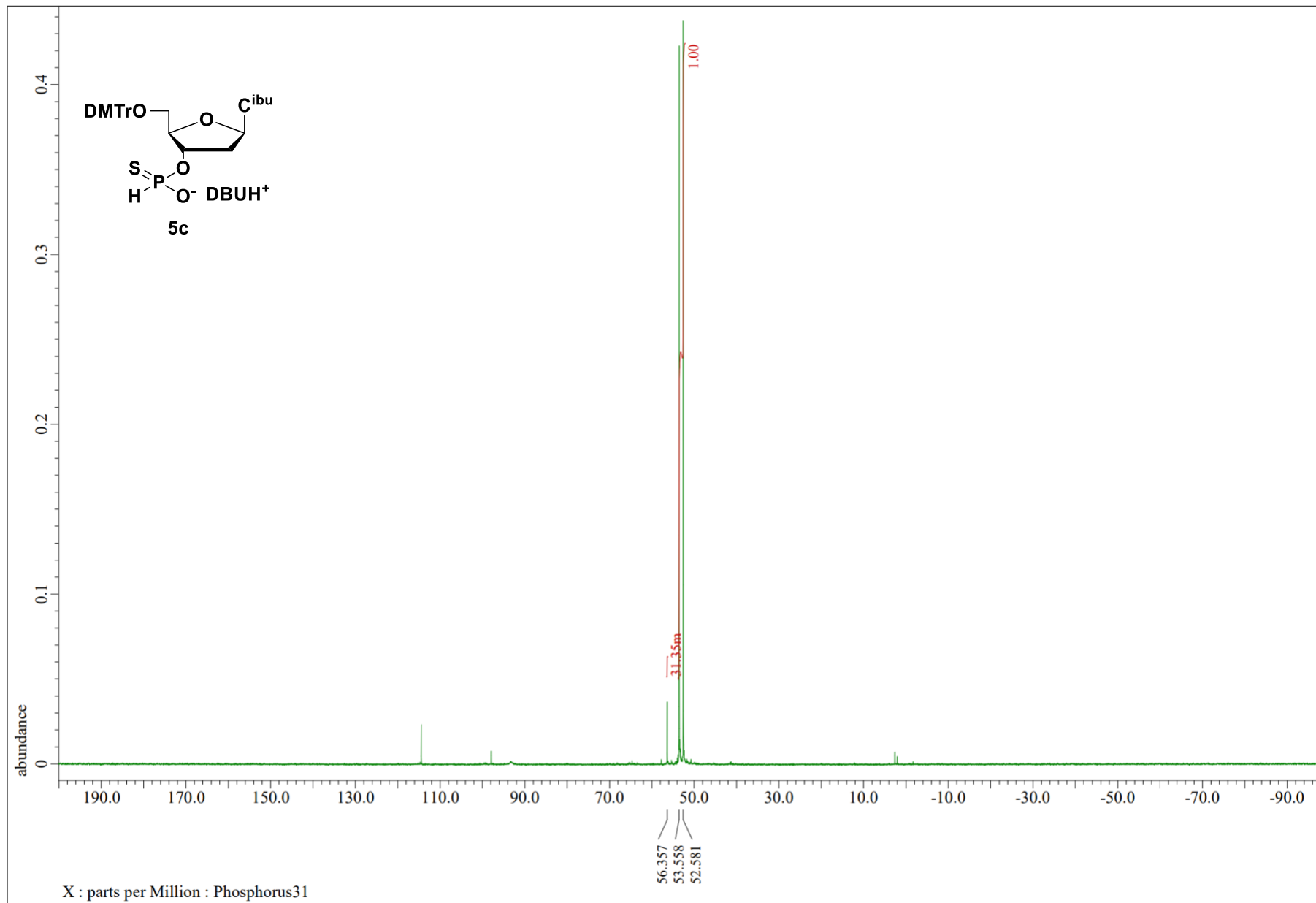


¹H-NMR (400 MHz, CDCl₃)

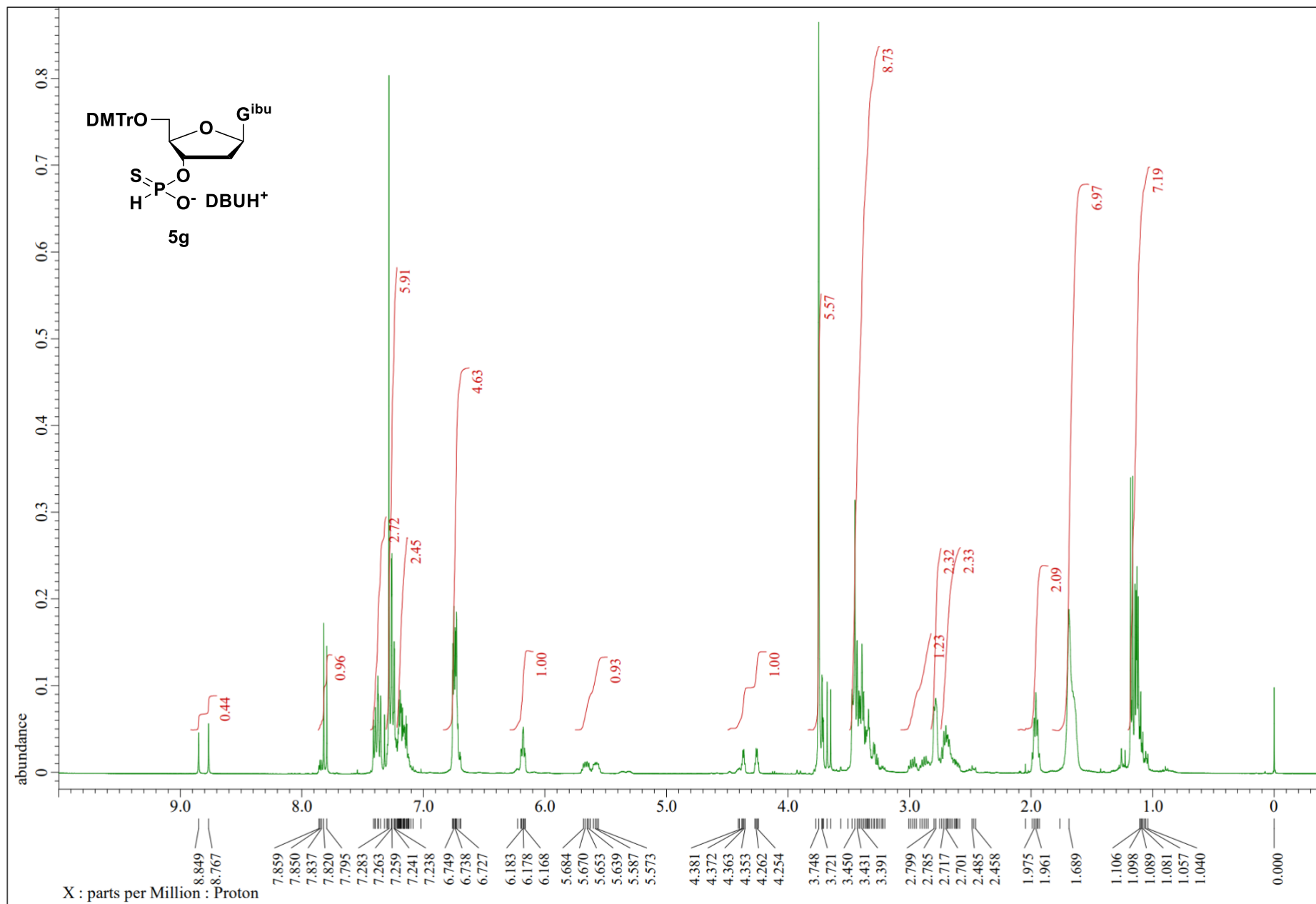




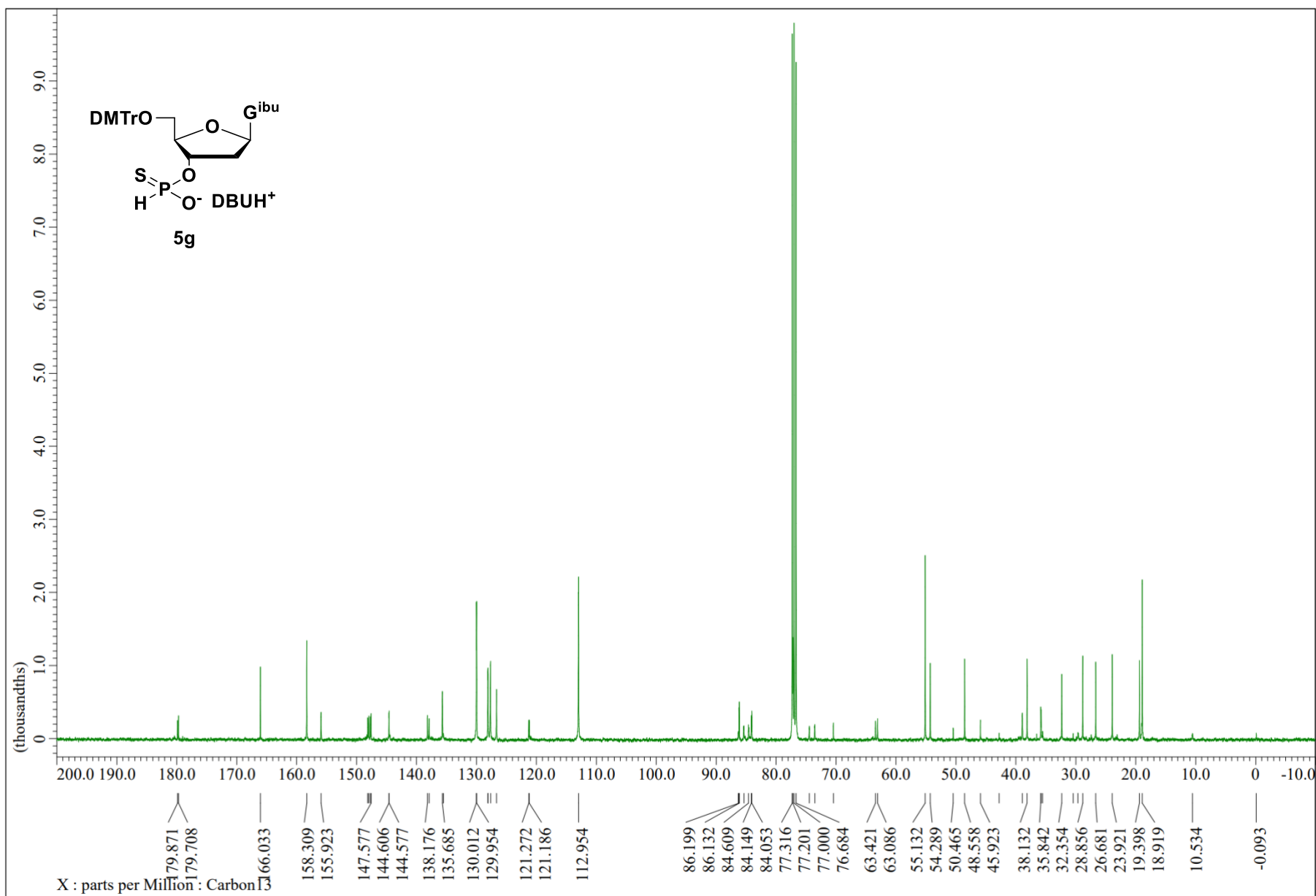
$^{31}\text{P}\{^1\text{H}\}$ NMR (162 MHz, CDCl_3)



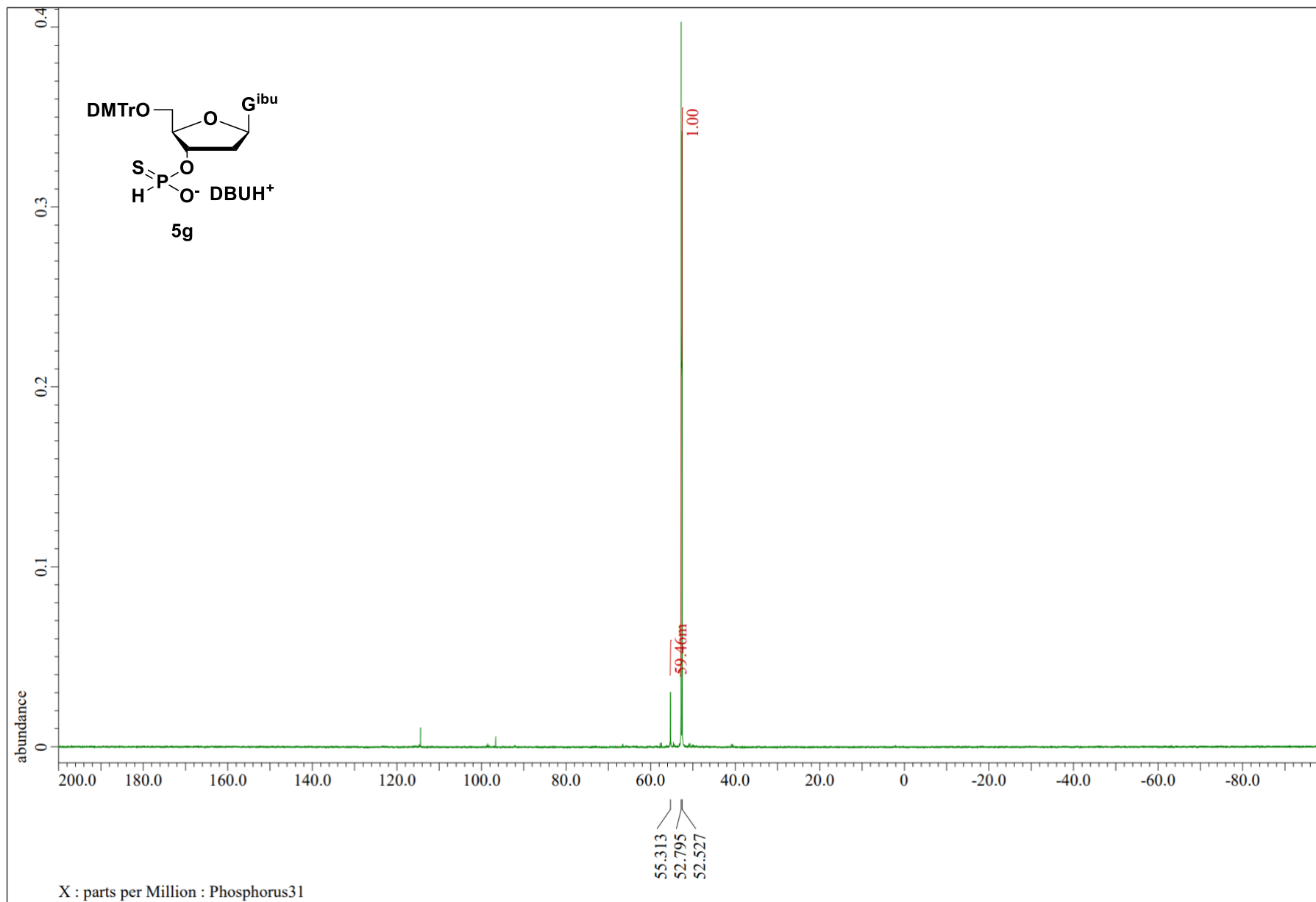
¹H-NMR (400 MHz, CDCl₃)



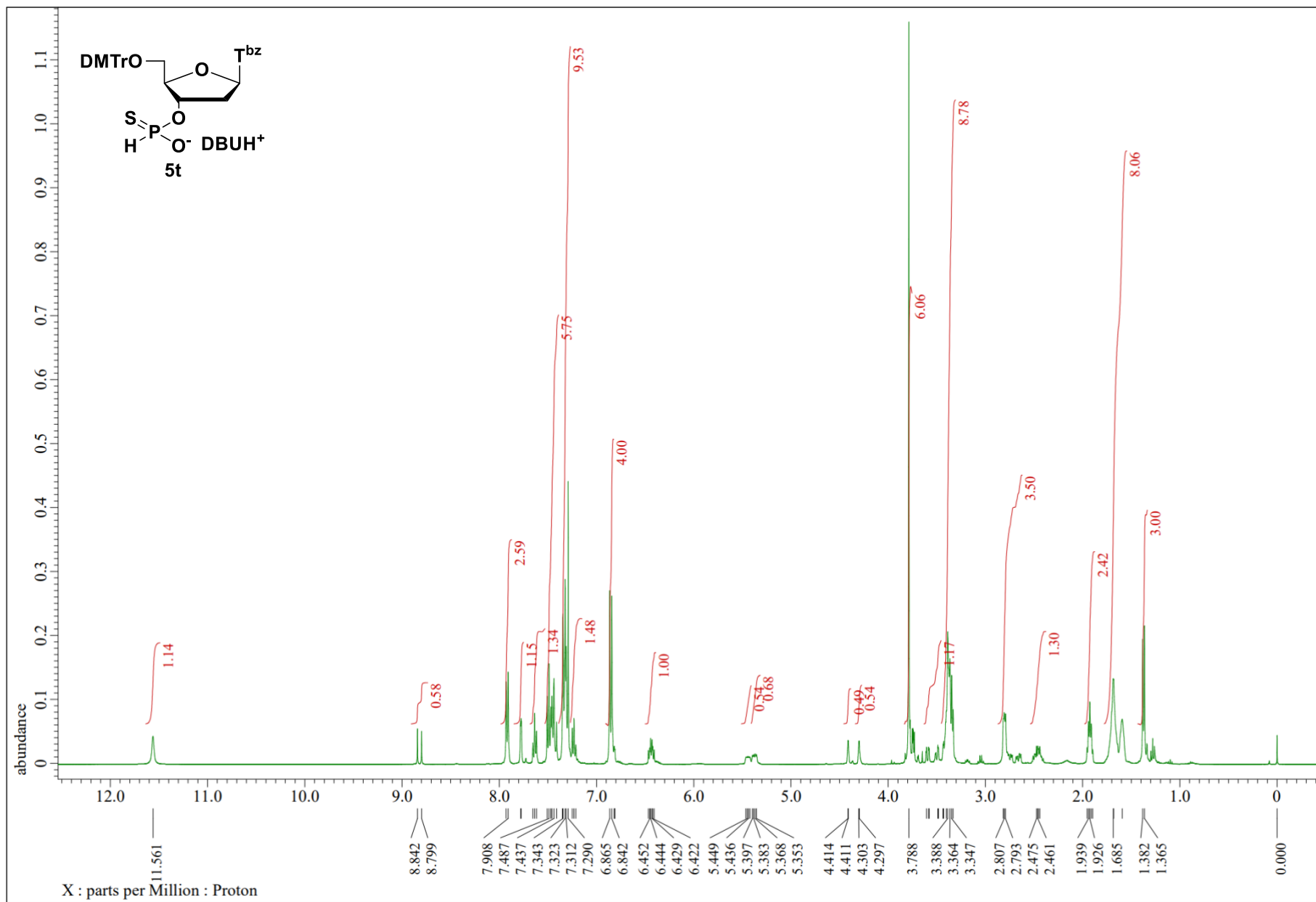
$^{13}\text{C}\{^1\text{H}\}$ NMR (100 MHz, CDCl_3)



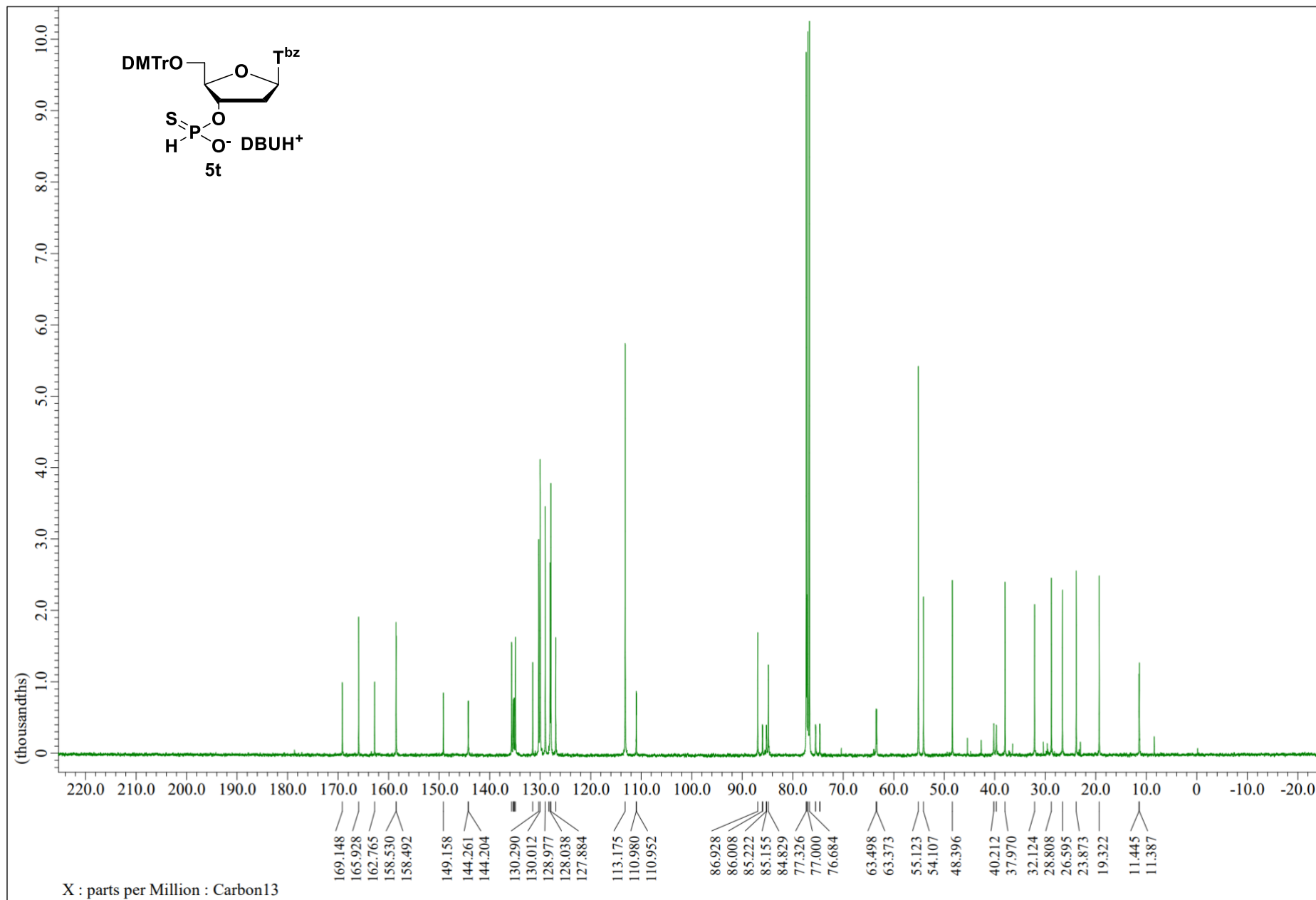
$^{31}\text{P}\{^1\text{H}\}$ NMR (162 MHz, CDCl_3)



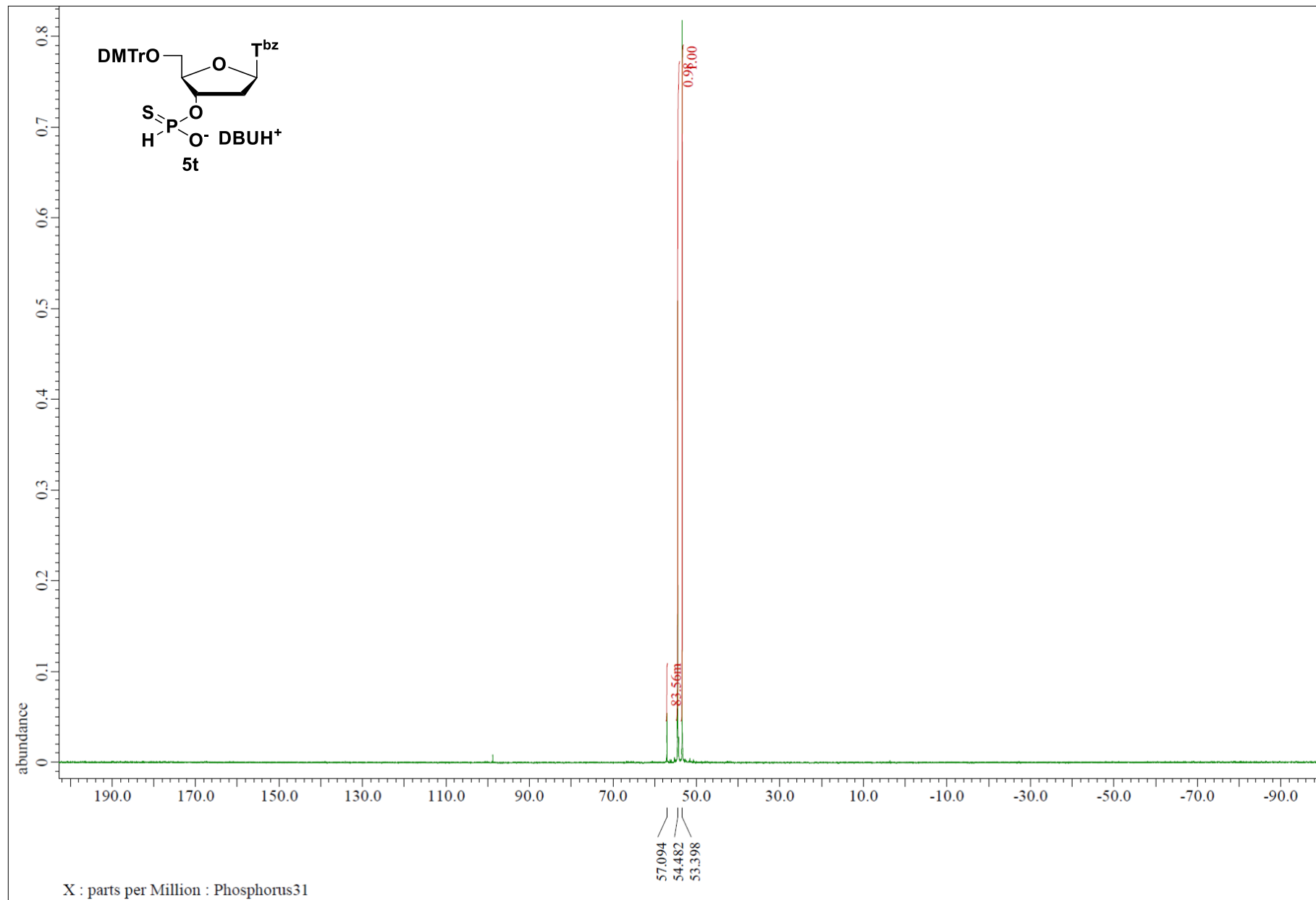
S35



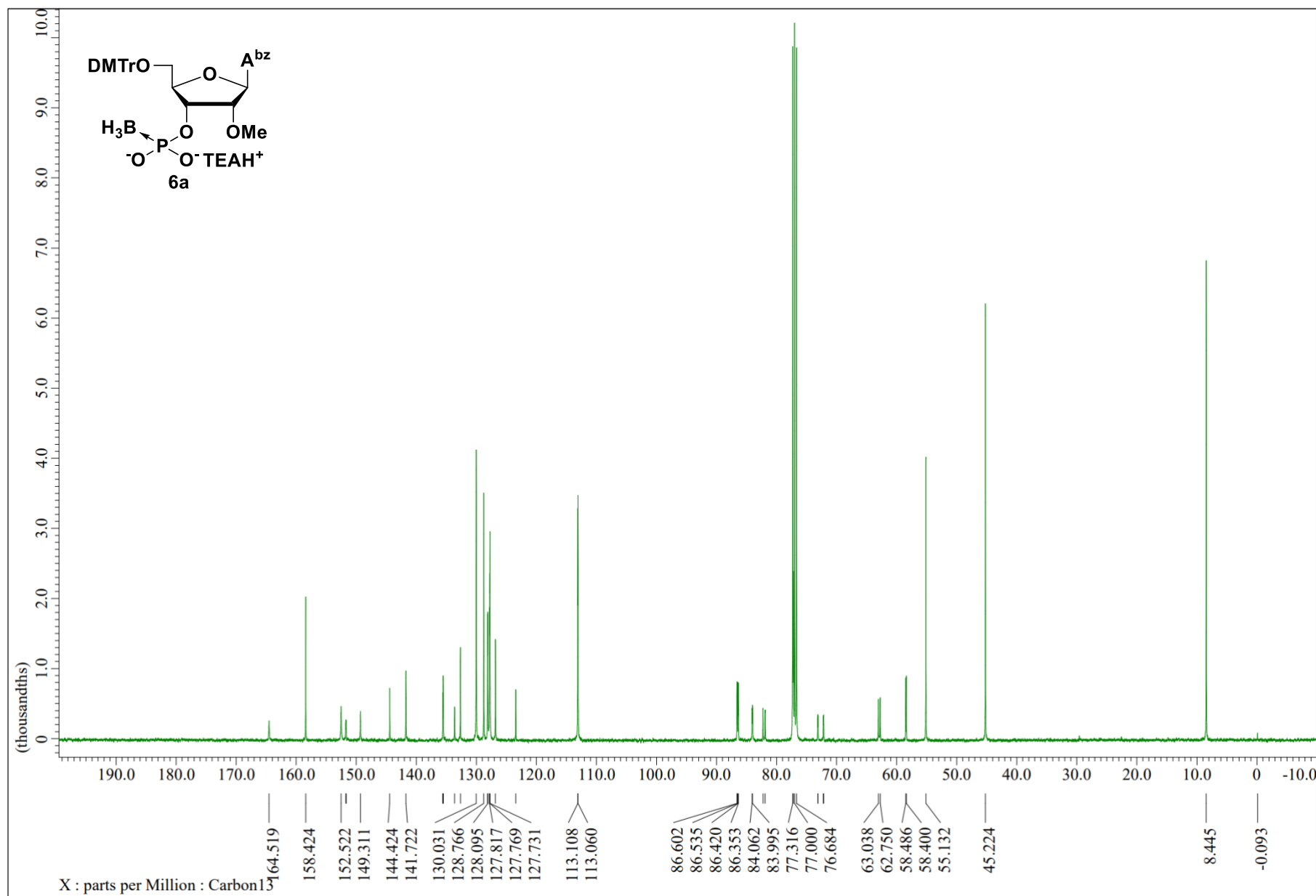
$^{13}\text{C}\{^1\text{H}\}$ NMR (100 MHz, CDCl_3)



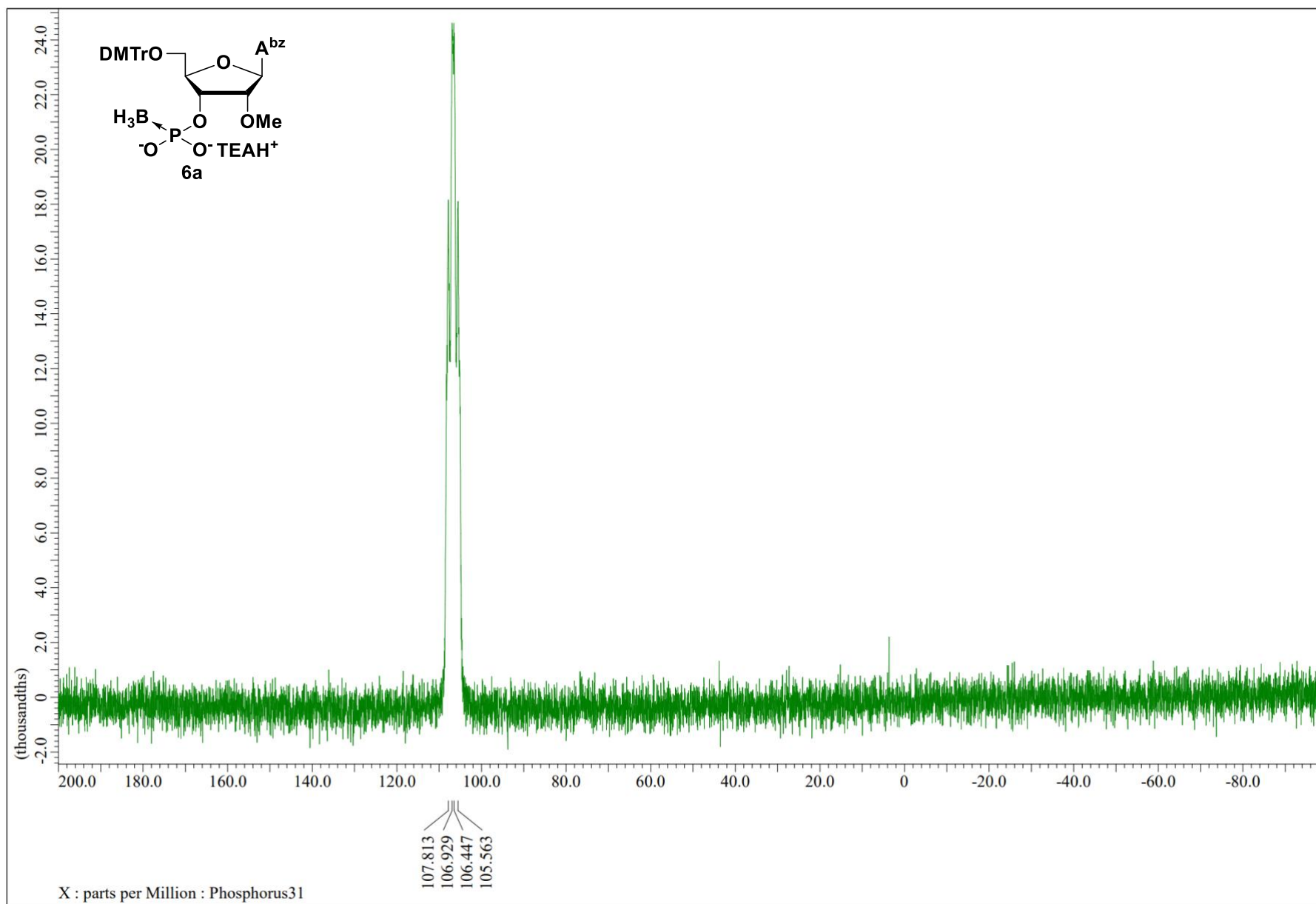
$^{31}\text{P}\{^1\text{H}\}$ NMR (162 MHz, CDCl_3)



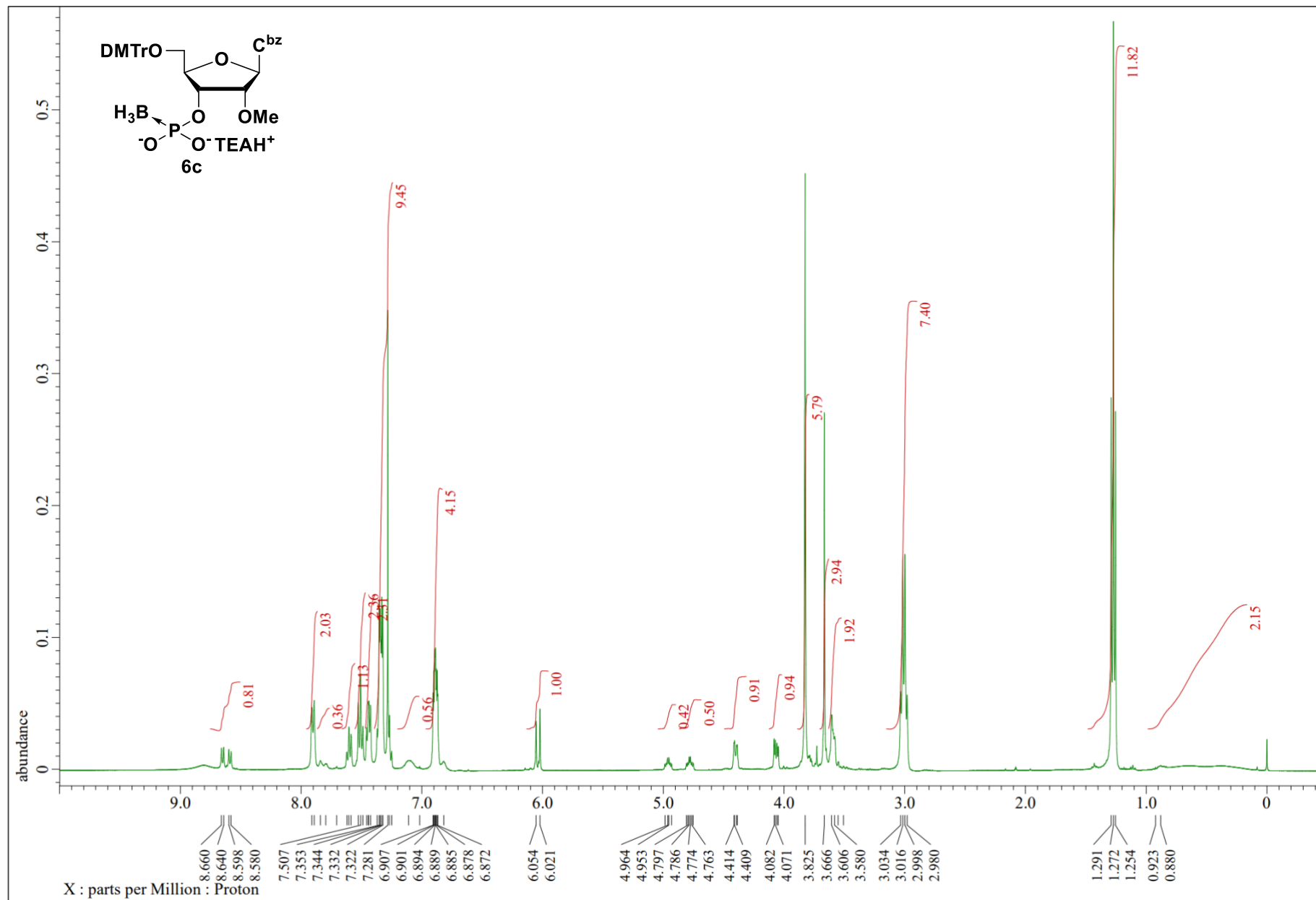
$^{13}\text{C}\{^1\text{H}\}$ NMR (100 MHz, CDCl_3)



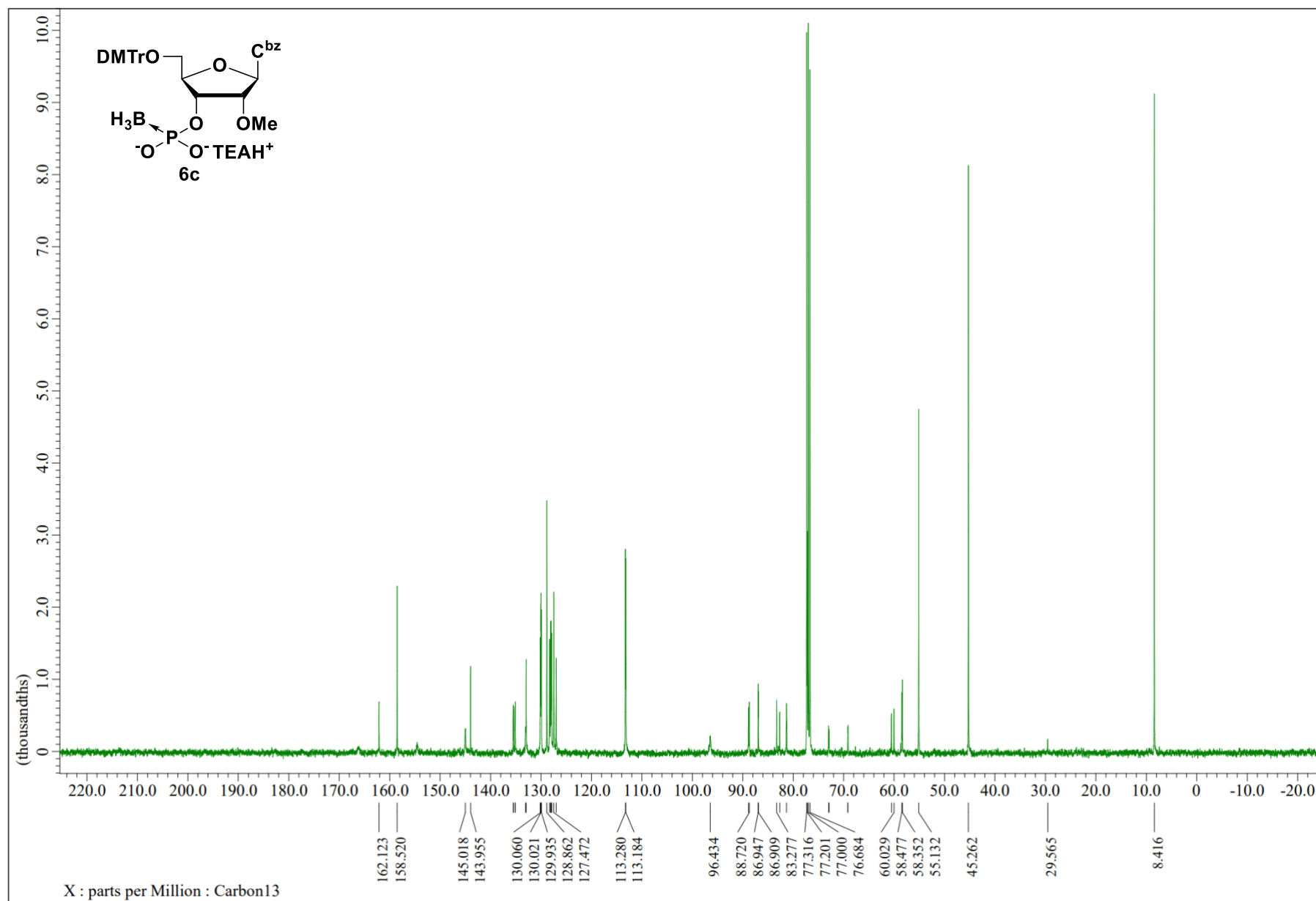
$^{31}\text{P}\{^1\text{H}\}$ NMR (162 MHz, CDCl_3)



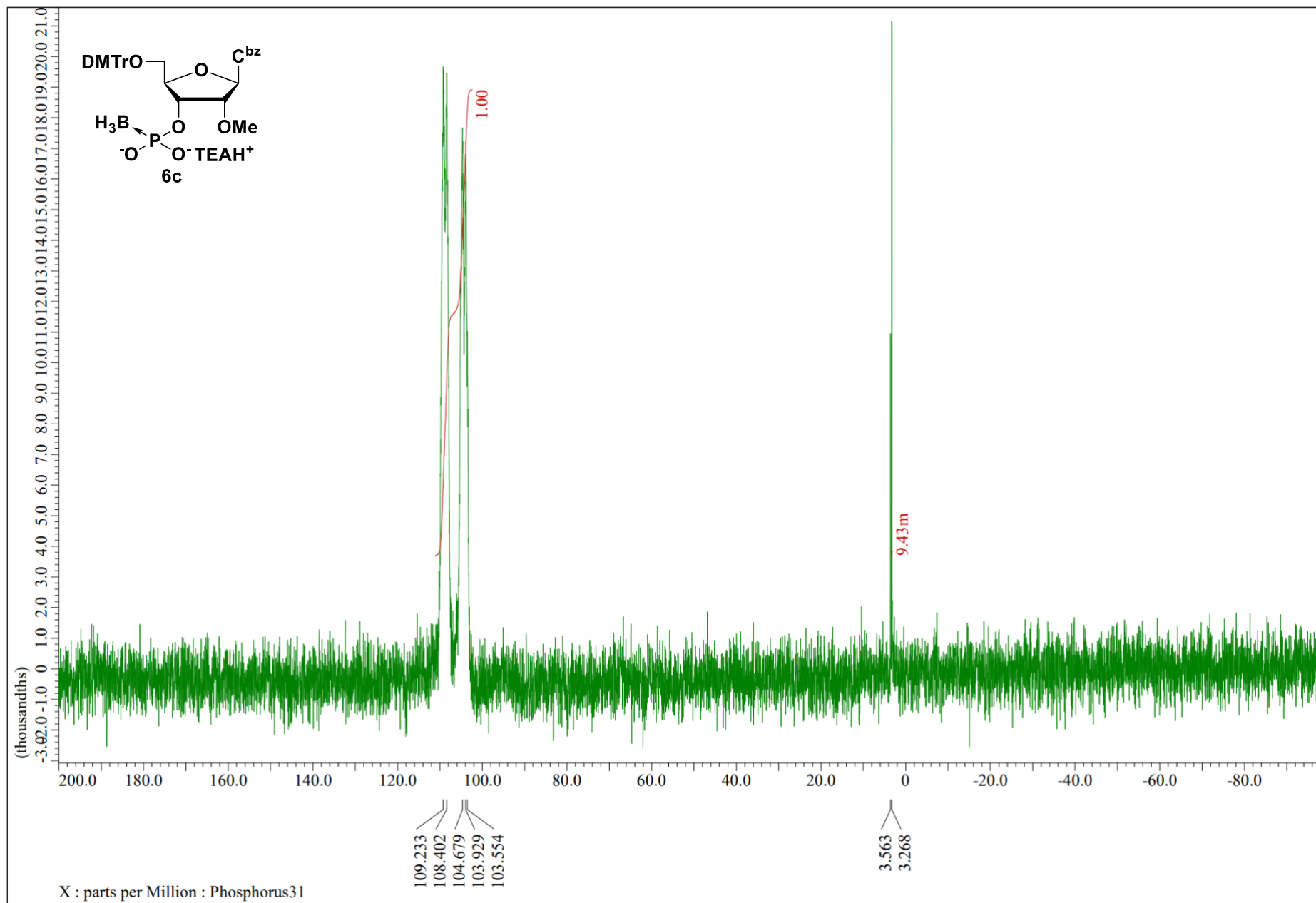
$^1\text{H-NMR}$ (400 MHz, CDCl_3)



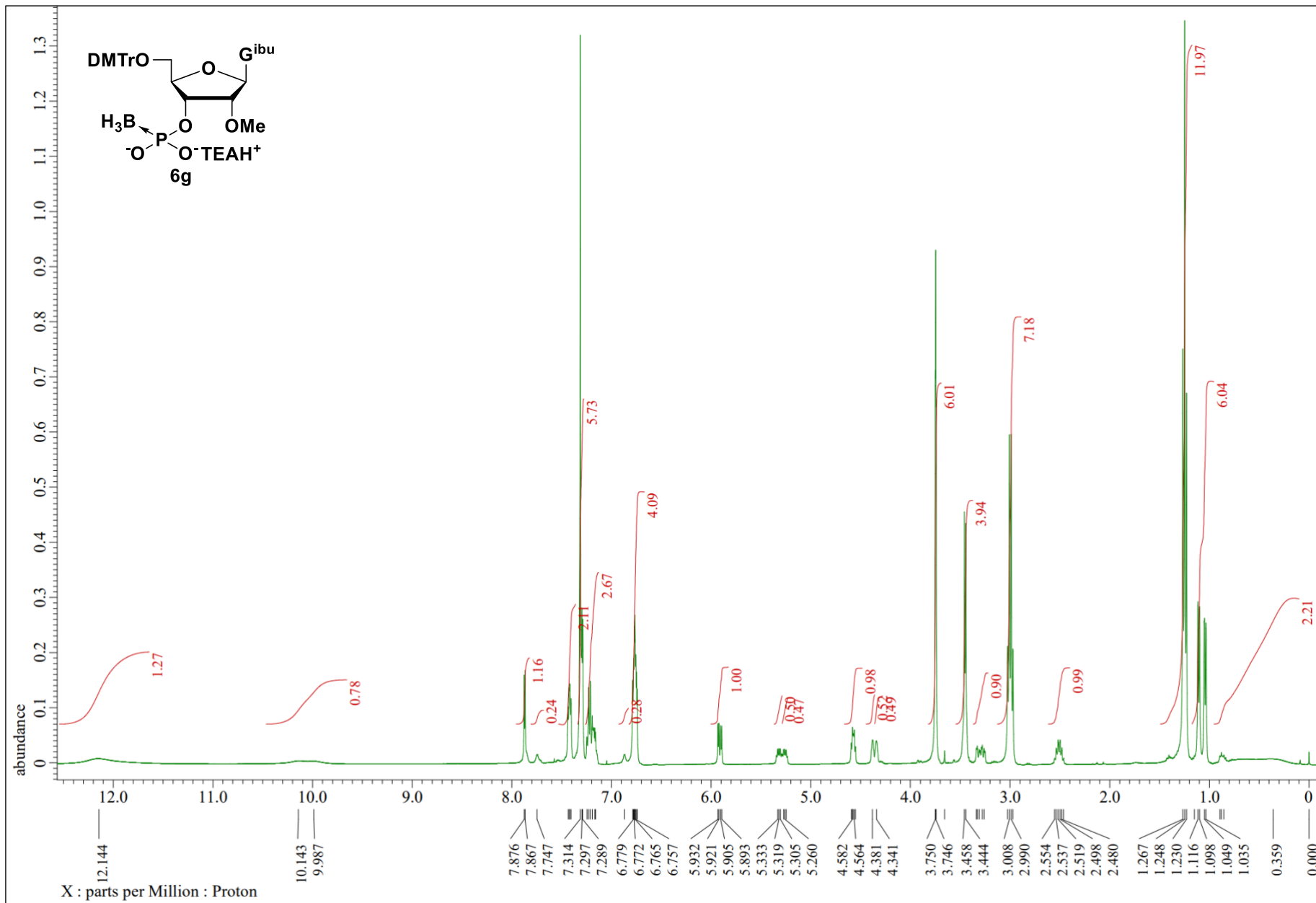
$^{13}\text{C}\{^1\text{H}\}$ NMR (100 MHz, CDCl_3)



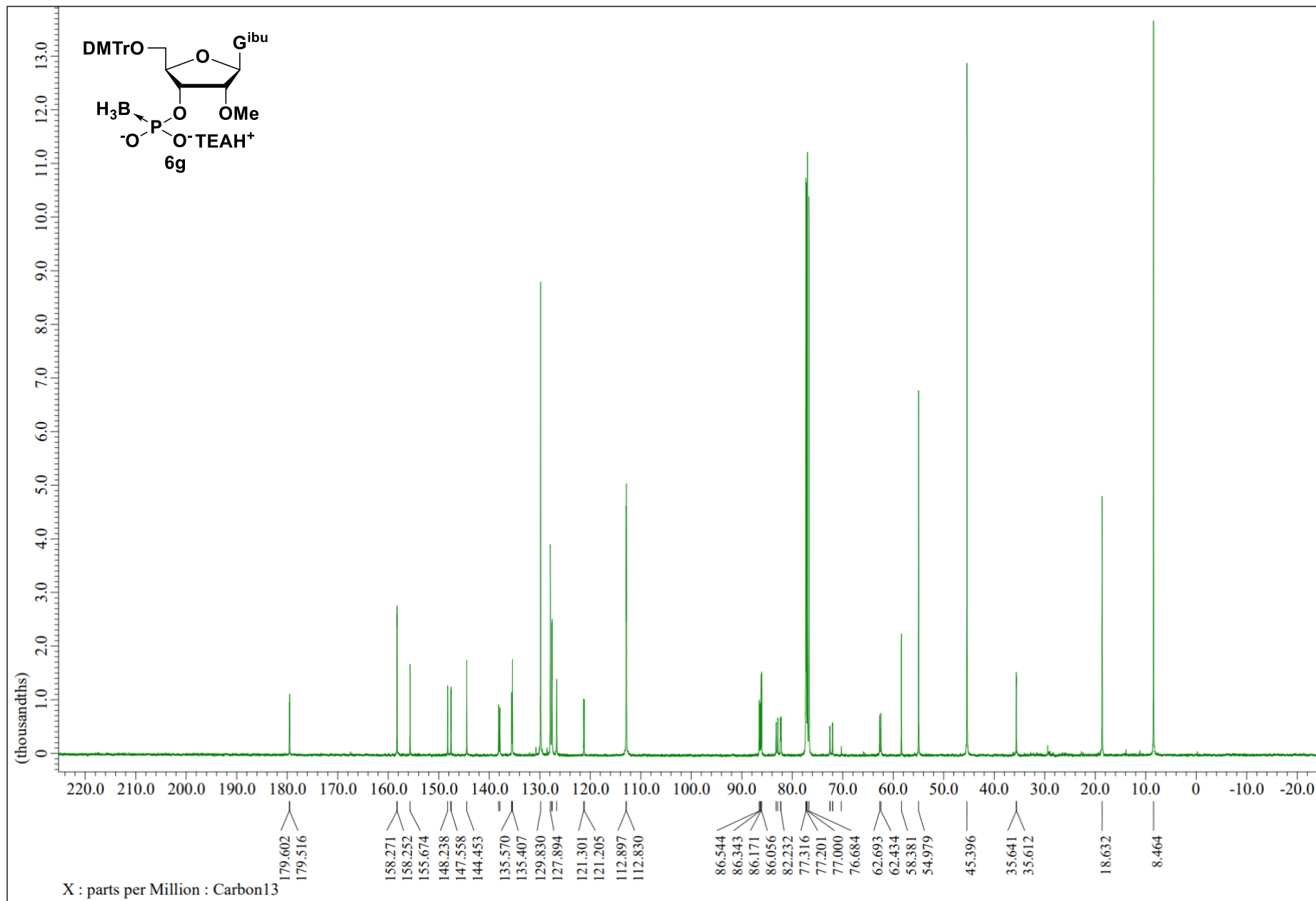
$^{31}\text{P}\{^1\text{H}\}$ NMR (162 MHz, CDCl_3)



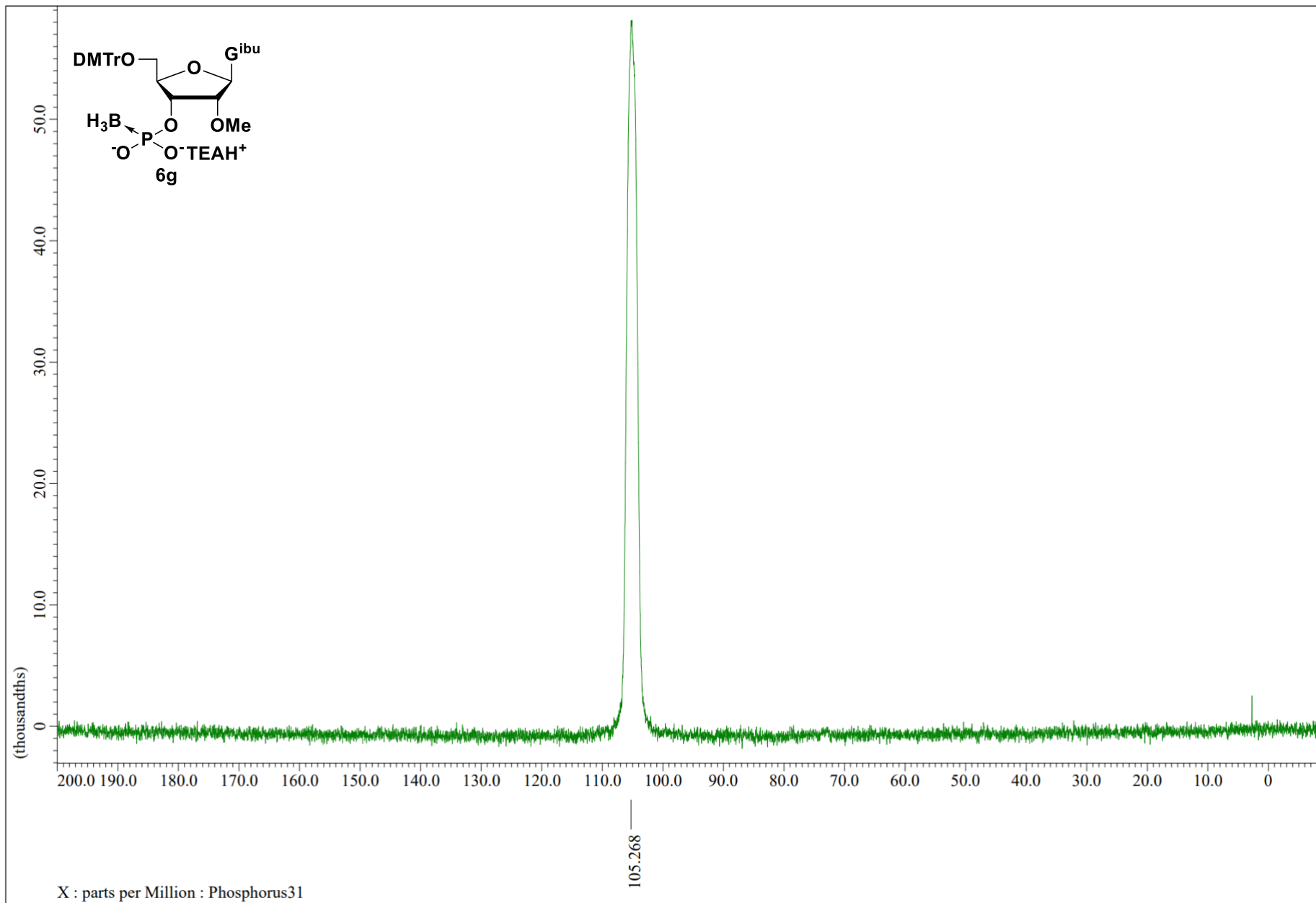
$^1\text{H-NMR}$ (400 MHz, CDCl_3)



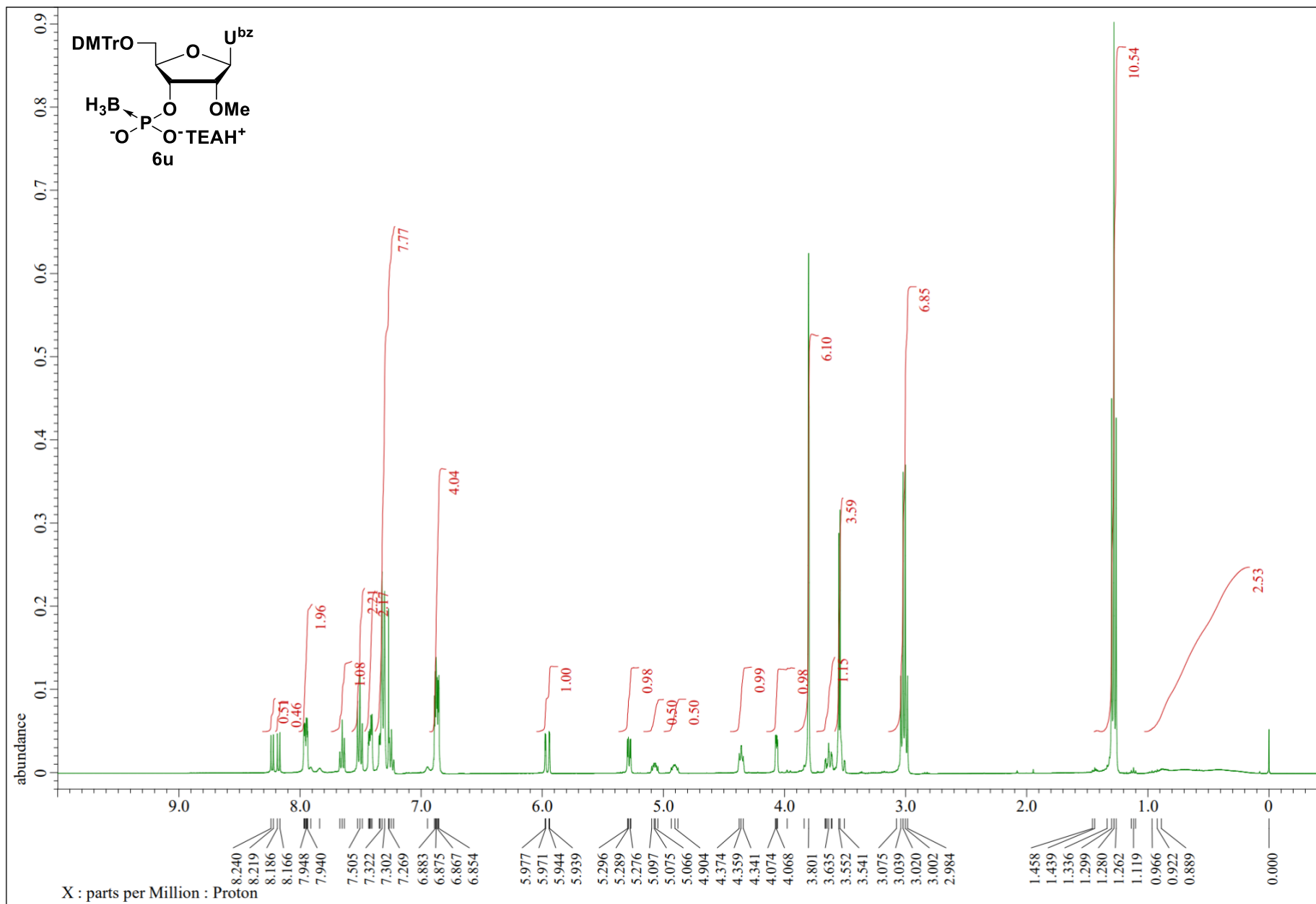
$^{13}\text{C}\{^1\text{H}\}$ NMR (100 MHz, CDCl_3)



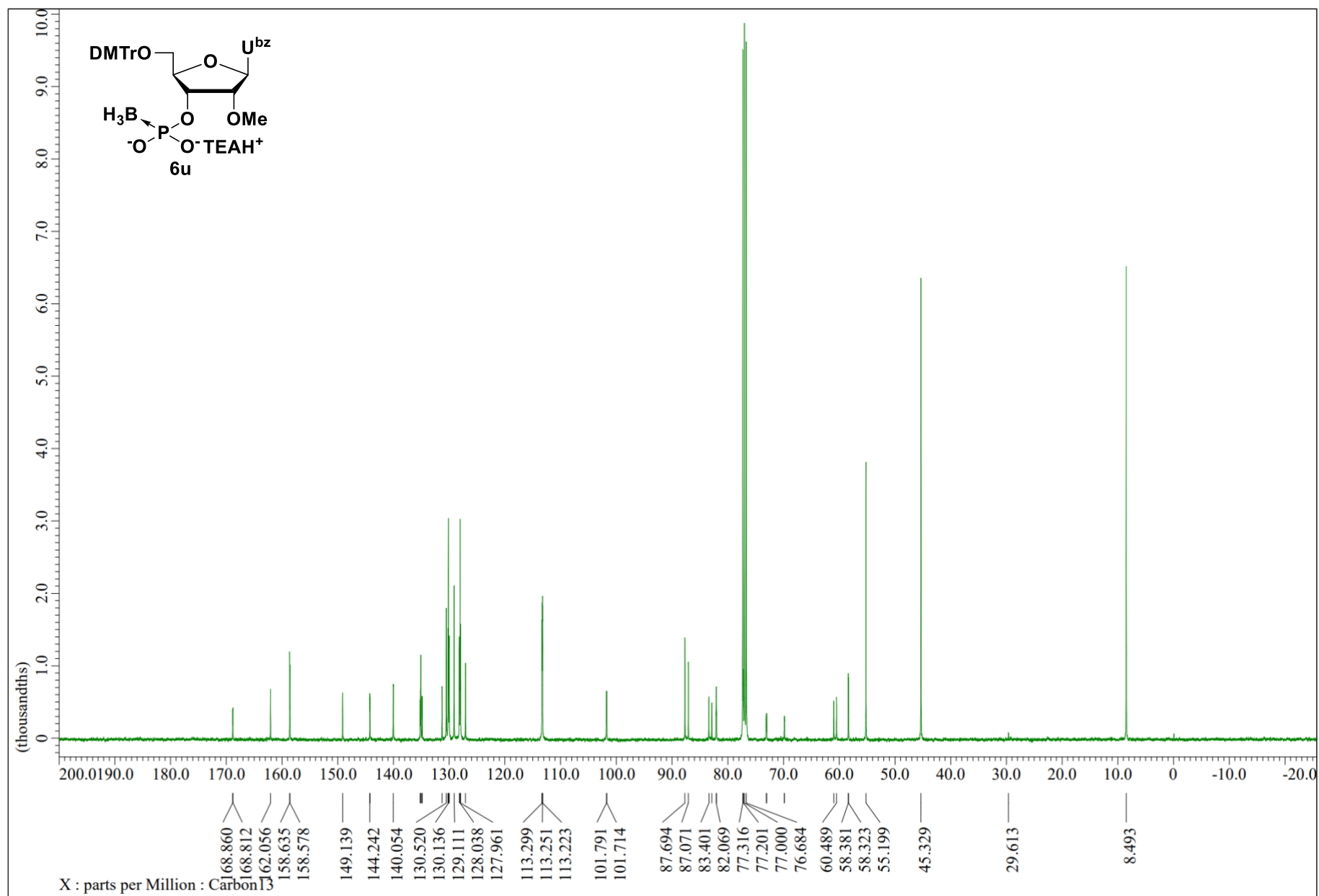
$^{31}\text{P}\{^1\text{H}\}$ NMR (162 MHz, CDCl_3)



¹H-NMR (400 MHz, CDCl₃)



$^{13}\text{C}\{^1\text{H}\}$ NMR (100 MHz, CDCl_3)



$^{31}\text{P}\{^1\text{H}\}$ NMR (162 MHz, CDCl_3)

